

## **Distribution Agreement**

In presenting this thesis or dissertation as a partial fulfillment of the requirements for an advanced degree from Emory University, I hereby grant to Emory University and its agents the non-exclusive license to archive, make accessible, and display my thesis or dissertation in whole or in part in all forms of media, now or hereafter known, including display on the world wide web. I understand that I may select some access restrictions as part of the online submission of this thesis or dissertation. I retain all ownership rights to the copyright of the thesis or dissertation. I also retain the right to use in future works (such as articles or books) all or part of this thesis or dissertation.

Signature:

---

Stephen Carter Frazier

---

Date

# How to Make a Giant Bubble

By

Stephen Carter Frazier  
Master of Science

Physics

---

Justin Burton  
Advisor

---

Connie Roth  
Committee Member

---

Alessandro Veneziani  
Committee Member

---

Eric Weeks  
Committee Member

Accepted:

---

Lisa A. Tedesco, Ph.D.  
Dean of the James T. Laney School of Graduate Studies

---

Date

# How to Make a Giant Bubble

By

Stephen Carter Frazier  
B.Sc., University of Georgia, 2014

Advisor: Justin Burton, PhD

An abstract of  
A thesis submitted to the Faculty of the  
James T. Laney School of Graduate Studies of Emory University  
in partial fulfillment of the requirements for the degree of  
Master of Science  
in Physics  
2016

## Abstract

### How to Make a Giant Bubble

By Stephen Carter Frazier

Soap and water solutions can form massive, free floating films encompassing volumes in excess of  $20 \text{ m}^3$  with thicknesses of only 10-100 microns when mixed with polymeric additives. These films are interesting from a physical standpoint due to their long lifetime and stability in ambient environments. We have investigated a variety of mixtures which are deemed “optimal” for making large bubbles, such as solutions made from guar seeds and polyethylene oxide (PEO). Using a combination of shear rheology, drop-based extensional rheology, high-speed studies of bursting mechanics, and drainage rate measurements, we found that “optimal” solutions showed similar extensional properties even though their shear viscosity differed by more than an order of magnitude. Polymeric bubbles also showed increased stability to aging in dry environments. Most importantly, it was found that soap and water solutions with polymers added lived 2-3 times longer and drained more slowly than typical soap and water solutions. These results show that the addition of polymers make the formation of massive bubbles possible due to enhanced elongational characteristics and drastically lower drainage rates.

# How to Make a Giant Bubble

By

Stephen Carter Frazier  
B.Sc., University of Georgia, 2014

Advisor: Justin Burton, PhD

A thesis submitted to the Faculty of the  
James T. Laney School of Graduate Studies of Emory University  
in partial fulfillment of the requirements for the degree of  
Master of Science  
in Physics  
2016

# Acknowledgements

The support and kindness I have received during the course of my studies here at Emory has been instrumental in the success I have experienced. I'm not certain that I will be able to put into words the gratitude I feel towards everyone who has helped me along the way, but I will attempt to express my deepest thanks here.

Without the invaluable support, guidance, and knowledge provided by my excellent advisor Dr. Justin Burton, I certainly would not have reached this point in my studies. Since I began working in your lab as a rotation student, your passion for your work has been evident and infectious. Your excitement about science in general has also lead to my own increased enthusiasm for both my work and scientific issues in general. I also owe you a great deal of thanks for putting in all the time to help me edit my research projects and this thesis, as I know it has taken a great deal of time from your already very busy life. I have been privileged to watch this lab grow through your guidance, and I hope that the work that I have carried out under your direction has contributed to that growth.

Many thanks also go out to my committee members Eric Weeks, Connie Roth, and Alessandro Veneziani for helping me finish this thesis in a timely manner. Having four professors come together and take time to give me input on my work and guidance on my next steps has proven to be an immense help in my research. My interactions with each of you have also been consistently pleasant and enlightening, and I know you all have contributed to my success here. I thank you all for being so accommodating and for giving me the advice necessary to ensure that I carry out my work to a high standard.

In every stage of my thesis research I have enlisted the help of the machine shop and electrical staff. As such, huge thanks go out to Cody Anderson, Horace Dale, and

Lowell Ramsey. Without Cody and Horace being willing to handle all of my requests and building the devices used in my experiments, I would have been completely lost. Also, without Lowell lending his expertise in electronics, I would have been without a means of taking data at several points in my research, and I likely would have electrocuted myself.

The administrative staff of this department have also always been of the highest quality, and I'm certain that my time here at Emory would not have gone so smoothly without their attention to detail. As such, many thanks go out to Calvin Jackson, Barbara Conner, Susan Cook, and Paulette Evans. Additional thanks go out to Art Kleyman for always being willing to help me install random software on, and fix, my computer. Thanks also go out to Jason boss for helping keep my computer, and the entire Burton lab's computers running, as well as for all of the enlightening conversations and pizza eating contests.

I am also very indebted to some of the post-docs of the department, namely Justin Pye, Carlos Orellana, and Juan Jose Lieter-Santos. Justin's assistance with all manner of issues in the Burton lab as well as with helping me in formatting this thesis have been immensely useful for me. Carlos's instructions on how to use the rheometer in the Weeks lab were integral to my research, and Juan Jose's assistance with some of my earlier presentations helped improve the overall quality of my work.

My time with the students of the Burton lab has also been very memorable, and I'm sure that I will look back very fondly on it for a long time to come. Janna, Guga, Jiaqi, Clay, Xiaolei, Toyin, Lia, Nick, Rui, and anybody else who I may be missing all deserve my sincerest thanks for putting up with me and my experiments. I know that my setups often taken too much space in the lab, so for your patience and kindness I thank you.

For all of the friends who I have met along the way, I will be forever grateful. In particular, Michael Thees, Janna Lowensohn, and Katherine Overman have been instrumental in helping me remove stress and retain my sanity over the past several months. Their willingness to both help me professionally and personally has truly left a lasting impression on me, as I know few other people who would be willing to visit the gym or the bar with me as readily as these three. All of my other friends who I have spent time with or stayed connected with during my time here will always be remembered for their quirks, kindness, and talents (Tyler, Nick, Donna, David, Anna, Cameron, Jacob, and Skye, just to name a few). I can honestly say that I cherish the time I have spent with you all.

As for my family, I owe you all more thanks than I can express. To my parents, I thank you for raising me to become the person that I am. All of your guidance throughout my life, and support while I have been at school, has meant the world to me. To Beth and Dan, thank you both for being a great sister and brother in law, and I am overjoyed for both of you for recently having Sadie and Jacob, as I know you will be great parents to them. To Chris, I am proud of how much you have accomplished lately, and I wish you the best of luck at your new store. To the rest of my family, as well as the Hamilton family, I thank you all for your love and support while I have been completing my studies. I know they have taken a lot of the time which I would have preferred to spend with you all, so I look forward to making up for all of that in the near future.

Last, but certainly not least, I want to thank Madison. You have been with me through this entire process from start to finish, and you have been an amazing constant in my life. I am so thankful that whatever error happened to put me into Latin class in high

school occurred, as it allowed me to be with you. I am beyond thankful that you have stuck with me through all these years, and I am immeasurably proud of the person you have become. With your determination and brilliance, I know that you will go on to do great things, and I consider myself privileged to get to be with you while you change the world. Thank you for helping to keep me young when everything seems to want to age me well beyond my years. I can't wait to see what our next big adventure is, and I am glad that I get to go into the real world with you by my side.

To all those who I have met on the path that has led me here, thank you.

# Table of Contents

## **Chapter 1: Introduction.....1**

1.1 Basics of Surfactant Solutions.....	2
1.2 Rheology Introduction.....	5
1.3 Mechanics of Film Formation and Bursting.....	7
1.3.1 Extensional Flow.....	7
1.3.2 Bursting Mechanics.....	8
1.4 Drainage.....	9
1.5 Soap Bubble Wiki.....	10
1.6 Thesis Outline.....	12

## **Chapter 2: Rheological Studies of Polymer-Surfactant Solutions.....13**

2.1 Introduction.....	13
2.2 Methods.....	14
2.2.1 Sample Preparation.....	14
2.2.2 Rheological Methods.....	15
2.3 Results and Discussion.....	16
2.4 Conclusion.....	18

## **Chapter 3: Extensional Flow and Bursting Mechanics of Polymer-Surfactant Films.....19**

3.1 Introduction.....	19
3.2 Methods.....	20
3.2.1 Extensional Flow.....	20
3.2.2 Bursting Mechanics.....	21
3.3 Results and Discussion.....	23
3.3.1 Extensional Flow results.....	23
3.3.2 Bursting Mechanics Results.....	25
3.4 Conclusion.....	28

## **Chapter 4: Drainage Profiles of Vertical Polymer Surfactant Films.....30**

4.1 Introduction.....	30
4.2 Methods.....	31
4.2.1 Sample Preparation.....	31
4.2.2 Thickness Measurement Methods.....	32
4.3 Results and Discussion.....	36

4.4 Conclusion.....	44
<b>Chapter 5: Summary.....</b>	<b>46</b>
5.1 Effects of polymeric additives on the drainage behaviors of soap films.....	46
<b>Bibliography.....</b>	<b>49</b>
<b>Non-printed sources.....</b>	<b>53</b>

# List of Figures

1	Figure 1.1: (Left) A typical bubble which can be made from a simple surfactant solution <sup>N2</sup> . (Right) An image depicting an industrial water treatment process <sup>N3</sup> .....	3
2	Figure 1.2: Drawing depicting a surfactant solution above the critical micellar concentration. The boundary layer has a large enough concentration of surfactants that all other surfactant molecules added will form clumps of micelles, as depicted by the circular grouping of molecules in the bulk of the liquid <sup>4</sup> .....	4
3	Figure 1.3: (Left) Diagram of a flat plate rheometer. The fluid sample is placed in between the Peltier plate and the upper geometry and exposed to different torques <sup>27</sup> . (Right) Photograph of rheometer used in this experiment.....	6
4	Figure 1.4: Qualitative descript of the typical behavior of Newtonian, shear thinning, and shear thickening fluids.....	7
5	Figure 1.5: Cartoon depiction of both Poiseuille (above) and plug (below) flow. Poiseuille flow implies a parabolic drainage front due to the immobile liquid interface, while plug flow assumes that the boundary layer is mobile and thus drainage is uniform.....	9
6	Figure 2.1: Visual approximation of bubble solution being pulled away from a string during film formation. The rope radius is $r$ , the velocity of the rope relative to the fluid is $v$ , the film thickness is $\delta$ , and the distance over which this velocity is achieved is $2r$ .....	16

7	<p>Figure 2.2: Viscosity vs. shear rate graph for control, glycerol, guar, and PEO samples. All guar samples are black, the two PEO samples are green, the glycerol sample is blue, and the control sample is red. All guar samples display at least a small degree of shear thinning over the observed range of shear rates.....17</p>
8	<p>Figure 3.1: Example photograph of a hanging droplet just prior to its tail pinching off.....21</p>
9	<p>Figure 3.2: Diagram of the apparatus used in the film rupture experiments. The camera recorded footage from one side of the enclosure, and a high power light was placed on the other side of the enclosure behind a diffuser to facilitate better image contrast.....22</p>
10	<p>Figure 3.3: Sample screen shot of a frame in which the diameter of a hole in a ruptured bubble was measured. The diameter of the hole was measured every 3 frames for each bubble, for the first 60 frames.....23</p>
11	<p>Figure 3.4: From left to right: Soap and water control, 0.3 g/L commercial PEO solution, 2.4 g/L guar solution, 4.5 g/L guar solution, and 1.0g/L PEO solution.....24</p>
12	<p>Figure 3.5: Graph depicting the average burst velocities of each sample. The black bars show the burst velocity for all solutions at 30 seconds, while the red bars show the burst velocities for all solutions at 10 minutes. PEO and soap solutions burst significantly faster than the more viscous guar and glycerol solutions.....26</p>
13	<p>Figure 3.6: Average stationary bubble lifetimes for the soap and water control and optimal guar and commercial PEO concentrations. The less viscous PEO solutions exhibit longer average lifetimes than the more viscous guar solutions. Error bars represent 95% confidence over 3 trials for each solution.....28</p>

14	<p>Figure 4.1: (Left) Image of the custom made spectrometer without the aluminum reflective plate in place. The screw post in the image was used to easily adjust the height of the platform, the black fan is the optical chopper, and the metal cubes next to the screw post and behind the chopper are the photodiode resistor and IR LED, respectively. (Right) The same device, with the aluminum reflective plate in place.....33</p>
15	<p>Figure 4.2: A circuit diagram of a voltage divider with a blocking capacitor. In this case, <math>V_{in}</math> is 18.0 V, <math>R_1</math> is 1 M<math>\Omega</math>, <math>R_2</math> is the voltage of the photodiode resistor (1 M<math>\Omega</math> <math>\pm</math> variations), <math>R_L</math> is the resistance of the lock-in amplifier (10 M<math>\Omega</math>), C is 20 <math>\mu</math>F, and <math>V_{out}</math> is measured by the lock-in amplifier.....34</p>
16	<p>Figure 4.3: Set of graphs depicting the change in voltage with respect to time for all heights and trials using the 0.5 g/L PEO and 4% by weight soap solution. As can be seen qualitatively from the pictures, the drainage rate gradually increased with height. The initial and final voltage drops correspond with the times at which the films first blocked the IR beam and when they popped, respectively.....37</p>
17	<p>Figure 4.4: Set of figures showing the normalized thickness vs. time data after Eq. 4.3 was applied to it. For each of the 11 heights, the average thickness values were calculated at each time, and a linear fit was applied to the resulting set of points.....38</p>
18	<p>Figure 4.5: Chart depicting the average lifetime for films made by each solution. The four longest lived solutions all have dish soap as their active surfactant, while the shortest lived solutions contain varying amounts of SDS. Average lifetimes</p>

	were calculated over all 55 trials for each solution, and error bars represent 95% confidence.....	39
19	Figure 4.6: Separate initial thickness profiles for each type of solution, with error bars denoting 95% confidence. As the graphs show, there is no significant difference between initial thicknesses when polymers are added to the solutions, either for soap solutions or SDS solutions. Vertical height was plotted on the x axis for ease of viewing.....	40
20	Figure 4.7: Graph depicting the thickness as a function of height for all solutions with soap as the active surfactant. While the solutions containing polymers may be slightly thicker, the difference is not significant compared to the error from the instrument.....	41
21	Figure 4.8: Graph depicting the thickness as a function of height for all solutions with SDS as the active surfactant. As above, the solutions containing polymers may be slightly thicker, but the difference is not significant compared to the error from the instrument .....	42
22	Figure 4.9: Graph of thickness vs. time for each polymer-soap solution at the maximum measured height. The soap and water solution (red) clearly drains much more quickly than the solutions containing soap and polymers. Error bars represent 95% confidence, and are obtained from the average of 5 measurements at each time point.....	43
23	Figure 4.10: Graph depicting the average bubble lifetime vs. average film lifetime for each solution. There is a good correlation between film lifetime and bubble lifetime, so the more robust a film of one solution is, the more robust its bubbles	

will be. The horizontal error bars represent 95% confidence over 55 trials, the vertical error bars represent 95% confidence over 5 trials.....44

# List of Tables

1 Table 3.1: Lists the maximum length attained by droplets of each solution as well as the surface tension of each solution. Once the PEO samples achieve a certain concentration, there appears to be a discontinuity in the maximum length the tails can reach.....25

# Chapter 1

## Introduction

The sight of an enormous soap bubble naturally invites human curiosity, for many reasons. Questions about what is added to the solutions, how the bubbles are able to become so large, and how the films are so stable often arise. The first of these questions is typically easy to answer, as there is often some type of polymer added to a soap and water mixture. The other two questions are much more difficult to answer, as there is not much literature on the subject and the dynamics of these large films are quite complicated, making them interesting from a physical point-of-view. As for industrial applications, there are several industrial processes which use surfactants and/or polymeric additives which create thick foams. If more is understood about these types of foams, then it may be possible to prevent the extreme buildup of foam in these procedures and therefore optimize processes.

There are many factors which may be at play in the formation of these large films, from surface tension gradients (Marangoni forces) and viscosity effects to drainage properties and self-healing abilities<sup>1</sup>. If all of these parameters are at favorable values, then it may be possible to create a free-floating soap film with a thickness in the range of tens of microns which encompasses very large volumes (the largest free-floating soap film was recently recorded at a size of  $23.3\text{m}^3$ )<sup>1</sup>. This seems unlikely based on conventional physical intuition, as a typical free floating soap film with no additives could only be expected to encompass a few cubic meters at most<sup>1</sup>. With all of these factors in mind, an in-depth examination of these solutions was carried out. Factors such as the solutions'

behavior under shear flow, their extensional characteristics, their bursting and aging mechanics, and their drainage properties were all investigated, in the hope of determining what mechanism allows these large films to form and become so stable.

In the course of this thesis, the rheological, extensional, bursting, and drainage properties of such polymer-surfactant solutions were studied in order to determine the mechanism which allows for these massive bubbles to form. The results of the experiments showed that polymer additives increase the average lifetimes of bubbles made from soap films without significantly increasing their thickness. Most importantly, it was shown that polymer-soap solutions also drain more slowly than typical soap and water films, making them much more stable than typical soap and water bubbles, even when extended to enormous lengths.

## **1.1 Basics of surfactant solutions**

When attempting to make a film or foam out of a liquid, better results may be achieved with a proper application of fluid mechanics principles. More specifically, with a proper understanding of things such as surfactants, polymers, surface tension, and viscosity, solutions which allow for larger and longer lived films and foams may be created. For instance, trying to make a bubble out of pure water is impossible, while adding a surfactant, such as soap, to the liquid completely alters the properties of the solution and its behavior, making foams and even large bubbles more likely to form. Figure 1.1 below depicts bubbles and foams which can be made with surfactants<sup>N2,N3</sup>.



Figure 1.1: (Left) A typical bubble which can be made from a simple surfactant solution<sup>N2</sup>. (Right) An image depicting an industrial water treatment process<sup>N3</sup>.

The reason that adding a surfactant works when attempting to make thin films and foams is that surfactants drastically lower the surface tension of water, thus making the solution more stable and “willing” to stretch. This is due to the fact that surfactants are amphiphilic, meaning that they are made of separate parts that would be immiscible if they weren’t connected<sup>2</sup>. More simply, surfactants have one end which is hydrophobic, and one end which is hydrophilic. The hydrophobic ends organize on the boundary of the liquid with the hydrophilic ends in the bulk, thus lowering the surface tension of the solution. This lower surface tension allows for the liquid to be more energetically stable when extended or agitated, leading to the creation of more robust films and foams<sup>2</sup>. If the concentration of surfactant in a solution is high enough, the surfactant molecules aggregate into clumps called micelles. At this critical micellar concentration (CMC), any additional surfactant added to the liquid goes into the micelles, which may also change the properties of the fluid, for instance by providing it with enhanced viscoelasticity<sup>3</sup>. Figure 1.2 below provides a drawing of a surfactant solution above the CMC, being drawn upward into a film<sup>4</sup>.

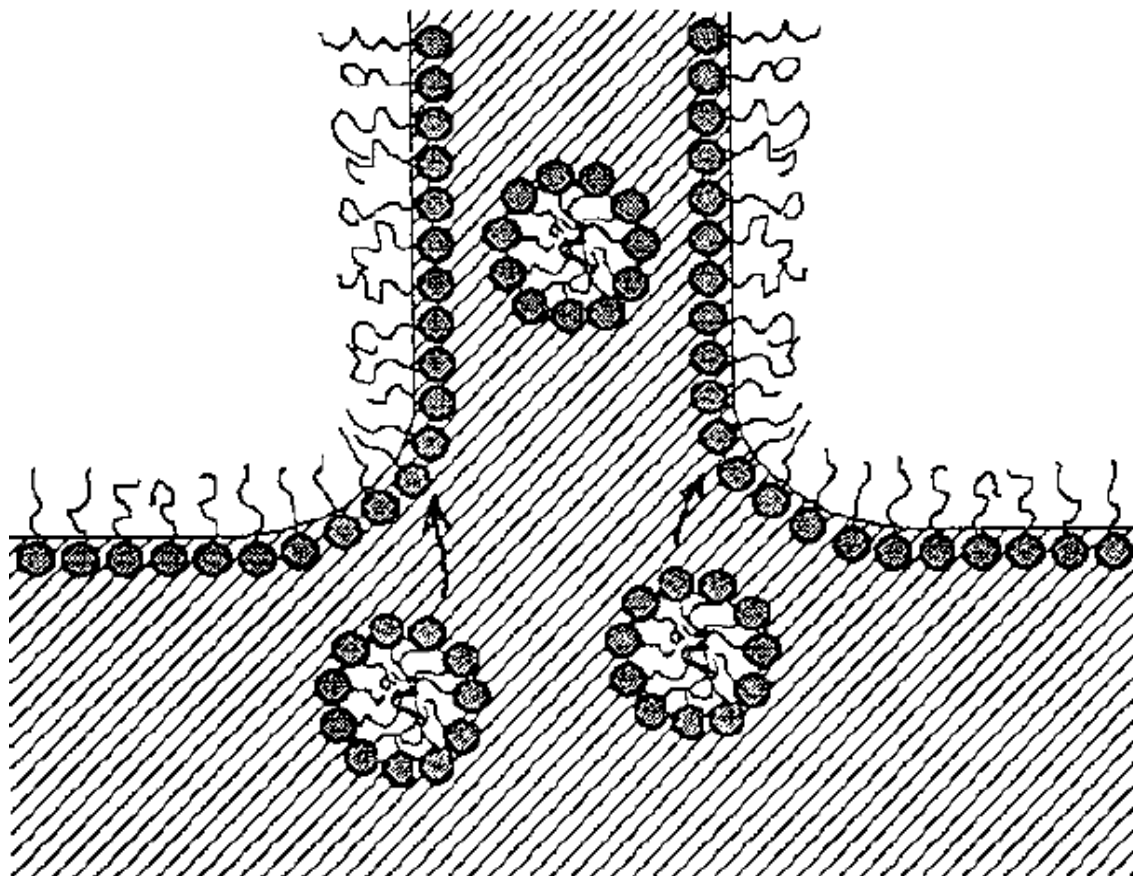


Figure 1.2: Drawing depicting a surfactant solution above the critical micellar concentration. The boundary layer has a large enough concentration of surfactants that all other surfactant molecules added will form clumps of micelles, as depicted by the circular grouping of molecules in the bulk of the liquid<sup>4</sup>.

Due to their interesting properties and practical uses, there has been a great deal of research on surfactant films, as they provide a convenient means of examining quasi-2d systems and are used in myriad industrial and commercial processes<sup>4-26</sup>. Some authors have also examined the properties of these solutions when combined with varying concentrations of polymer additives, as are used in the giant bubbles which inspired this work<sup>22-26</sup>. As will be discussed in later sections, these polymer-surfactant solutions have been shown to display unique behaviors, which warrant deeper investigation.

## 1.2 Rheology Introduction

The actual process of blowing a bubble can in fact expose a bubble solution to high stresses and a variety of forces, and the response of the films to these forces can vary greatly depending on several characteristics of the solutions. One simple way to record several characteristics of a fluid is to examine its rheological behavior. Rheology, which is the study of the flow and deformation of materials, is a commonly used tool in soft matter research and engineering. Rheological data are taken with a rheometer, shown below in Figure 1.3, which is a high precision tool consisting of a temperature controlled lower plate and an “upper geometry”, which typically spins or bobs to apply a torque to a fluid sample, at which point several types of data may be recorded, such as viscosity, storage modulus, and loss modulus<sup>27, 28</sup>. For the rheometer used in this experiment, the upper geometry is lowered to a desired height, called the gap width, and a fluid sample is placed inside the gap. The upper geometry then spins or oscillates at a set velocity which is measured at the rim of the upper plate and the shear rate, which is the ratio of velocity to gap width, is recorded along with the viscosity (the ratio of the shear stress to the shear rate) and several other characteristics of the sample.

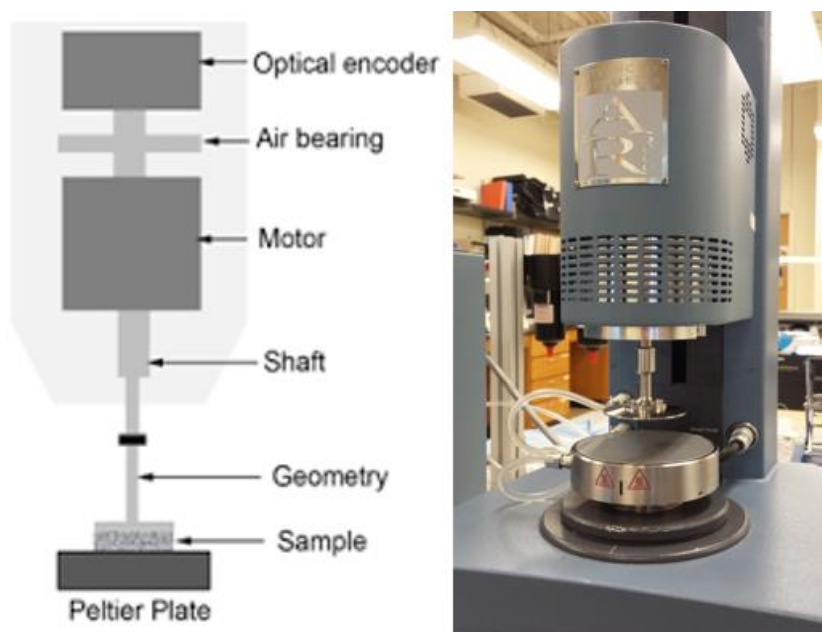


Figure 1.3: (Left) Diagram of a flat plate rheometer. The fluid sample is placed in between the Peltier plate and the upper geometry and exposed to different torques<sup>27</sup>. (Right) Photograph of rheometer used in this experiment, an AR2000 rheometer manufactured by TA Instruments.

One common type of rheometric measurement shows the viscosity as a function of shear rate. For many fluids, known as Newtonian fluids, these graphs are simply flat lines for most reasonable shear rates, meaning that those types of fluids have a viscosity which is independent of shear rate. Non-Newtonian fluids exhibit a changing viscosity with respect to shear rate. Examples of non-Newtonian fluids, which are often made up of a mixture of polymers or colloidal particles and water, include ketchup, which shear thins (has viscosity which lowers under increased shear), and corn starch in water, which shear thickens (has viscosity which rises under increased shear)<sup>27</sup>. Figure 1.4 below shows a qualitative graph depicting the typical behavior of shear thinning, shear thickening, and Newtonian fluids for moderate shear rates.

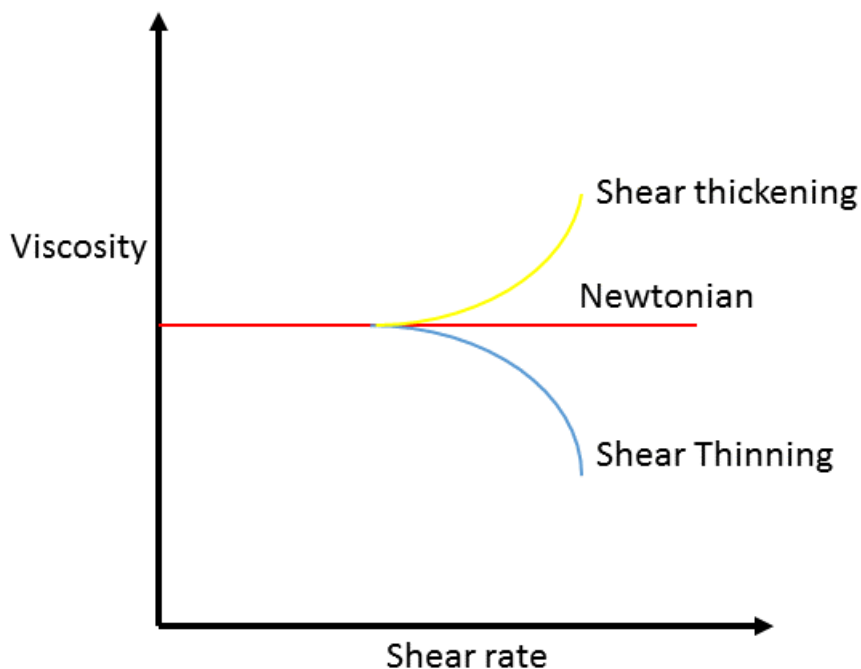


Figure 1.4: Qualitative description of the typical behavior of Newtonian, shear thinning, and shear thickening fluids.

## 1.3 Mechanics of film formation and bursting

### 1.3.1 Extensional Flow

The type of flow most directly related to the pulling and formation of a free floating soap film is called extensional flow, not shear flow. Shear flow is flow in which the solution's velocity gradient is perpendicular to the height of the sample (as is the case in rheometric measurements) while extensional flow occurs when particles in a solution are compressed together or pulled apart, leading to an elongational deformation of the material<sup>27</sup>. Since a bubble film is pulled away from the surface it is attached to (i.e. a rope or a bubble wand), it is useful to examine how a bubble solution behaves when exposed to this type of deformation. Some solutions may be able to extend great distances without breaking while others may hardly be able to extend at all. How far these films can extend

before rupture, as well as intrinsic qualities of the solutions such as viscosity and surface tension, can contribute to the overall size and stability of a bubble formed by the fluid<sup>29</sup>.

### *1.3.2 Bursting Mechanics*

Large polymeric bubbles display unique characteristics compared to those made by typical soap and water solutions; thus, it is useful to examine the behavior of the bubbles themselves, especially as they age and burst. Two main factors which contribute to the popping of bubbles are (1) drainage due to gravity and (2) evaporation of the film. This means that when bubbles are in humid environments, or are made of fluids that drain more slowly, they may favor longer lifetimes since these characteristics lead to lower levels of evaporation and slower drainage, respectively<sup>1,30</sup>.

One method of measuring the drainage of these films, as well as observing the stability of the films over time, is to let bubbles made from the solutions live for various times and then pop the bubbles and measure the burst velocity. Assuming low viscosity, the velocity of a retracting soap film is constant and can be predicted by the relation

$$v = \sqrt{\frac{2\gamma}{\rho\delta}}, \quad (\text{Eq. 1.1})$$

where  $v$  is the velocity of the retracting film,  $\gamma$  is the surface tension,  $\rho$  is the density, and  $\delta$  is the film thickness of the bubble<sup>3,31</sup>. Measuring all of these quantities can lead to an indication as to the degree of drainage experienced by these films (since the drainage rate influences the thickness), and may also help identify the existence of viscoelastic effects, which may be present if the retraction velocity is higher than that predicted by Eq. 1.1.

## 1.4 Drainage

When any liquid film is pulled upward from a bath without rupturing, it will begin to gradually drain until it becomes too thin to support itself and simply ruptures. Depending upon the makeup of the solution used to create the film, several types of drainage flows are possible. For polymer-surfactant solutions in particular, there is some debate over whether the drainage flow inside films is due to plug-type flow or Poiseuille flow. Plug flow is flow through a channel in which there is slip at the wall or boundary, while Poiseuille flow assumes that there is an immobile boundary layer which does not allow slippage<sup>1</sup>. Figure 1.5 below provides a drawing depicting the difference between these two types of flow.

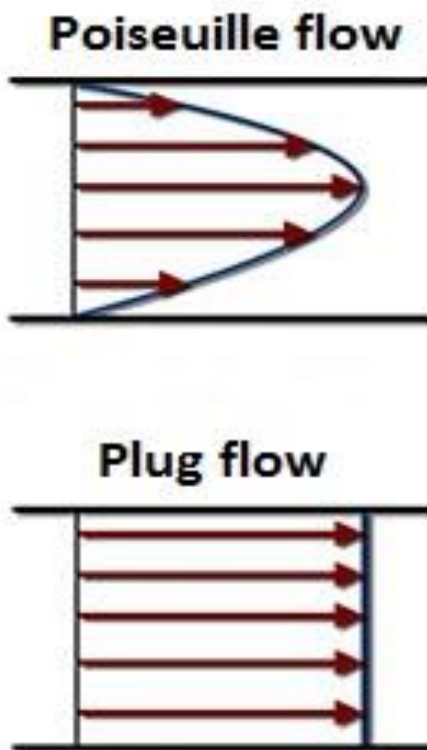


Figure 1.5: Cartoon depiction of both Poiseuille (above) and plug (below) flow. Poiseuille flow implies a parabolic drainage front due to the immobile liquid interface, while plug flow assumes that the boundary layer is mobile and thus drainage is uniform.

It is common practice, both in theory and experiment, to consider surfactant films as characteristically Poiseuille-type flow rather than plug flow<sup>6, 8, 9</sup>. This is due to the assumption that the surfactants in such films readily move towards the water-air interface in order to attain the most favorable orientation, given their amphiphilic nature. This leads to an immobile boundary layer coated in surfactant with their hydrophilic tails pointed inward, resulting in an immobile “wall” against which the draining solution will not slip. It should be noted that for polymer-surfactant solutions the drainage profiles may differ entirely<sup>22</sup>, as will be discussed later in this work.

## **1.5 Soap Bubble Wiki**

A great deal of the research outlined in this thesis found original inspiration through examination of the pages of the Soap Bubble Wiki, an online forum in which bubble enthusiasts discuss their favorite solutions for making giant bubbles. The site’s pages even list out recipes for solutions which its members have used to make giant bubbles. These recipes provided the basis for the solutions outlined in these experiments.

While the members of this website often have their own unique recipes when it comes to making giant bubbles, there seems to be a consensus that Dawn brand dish soaps are best for bubble formation. Due to this consensus, Dawn Pro dish soap was used as the primary surfactant in most of the films examined. In the later stages of this research another surfactant, sodium dodecyl sulfate (SDS), was used in order to examine the effect of the surfactant type on bubble characteristics as well as to have a more thoroughly researched surfactant than the proprietary Dawn formula.

Two of the polymer additives most commonly talked about on the website are guar gum and polyethylene oxide (PEO). Guar gum, powder derived from the seeds of the guar

plant, is a food additive used as a thickening agent. PEO, on the other hand, is a polymer which is often used as a lubricant. Sources for both of these polymers are given on the Soap Bubble Wiki, so these common commercial sources were investigated, in addition to more pure research quality sources ordered from Sigma Aldrich.

After much consideration, research quality guar gum powder, commercial PEO and research quality PEO were used. The research quality guar was chosen in order to minimize particulate matter in the bubble solutions, while commercial and research quality PEO were both examined in order to determine if polymer purity or molecular weight would have any effect on bubble quality, as will be discussed later. Research quality PEO was also chosen because the commercial PEO powder is a proprietary formula found in the veterinary lubricant powder Jlube. All that is known of this powder is that it is 25% pure PEO with a molecular weight given as over 2 million, with the other 75% of the powder being unspecified sugars. Thus, the research quality PEO used later in these experiments was a 98% pure, 2 million molecular weight sample purchased from Sigma Aldrich and used as delivered.

While a variety of concentrations of each polymer were examined, it should be noted that for both guar and PEO bubble solutions there is a generally accepted “optimal” concentration range listed on the Soap Bubble Wiki for both types of polymer. Thus, when creating the range of concentrations used for these experiments, solutions with concentrations both inside and outside of these ranges were studied. This range of concentrations made it possible to qualitatively and quantitatively study the characteristics of solutions which would produce the best bubbles compared to those which would be less effective.

## 1.6 Thesis outline

This thesis consists of 5 chapters detailing and summarizing the work completed in the pursuit of a Master of Science degree at Emory University.

Chapter 2 details the results of rheological measurements carried out on a variety of solutions. The information gleaned regarding the rheological properties of these solutions, including the shear viscosity of each, informed later decisions as to which solutions were most pertinent to examine. Data depicting the shear thinning behavior, when compared to the actual behavior of the films when formed into large bubbles, were used to examine the relationship between viscosity and bubble size.

Chapter 3 describes the measurements of the extensional properties of many of the solutions, as well as the bursting mechanics of each. The results of this section show that extensional flow and film drainage are intimately related to both the robustness of the bubbles and films as well as their size and average lifetimes. Information gleaned from these data provided clues as to what areas to examine next, namely the film drainage characteristics.

Chapter 4 explains the results of attempts to create full experimental drainage profiles of vertical polymer-surfactant films, something that is currently not to be found in the literature. Data recorded from a spectrometer constructed in-house provide profiles of several types of solutions with respect to both time and height. These data are also used in order to provide insight into which films may be the most effective in terms of yielding the longest lived and largest free floating bubbles.

## Chapter 2

# Rheological Studies of Polymer-Surfactant Solutions

### 2.1 Introduction

Rheological studies have long proven to be useful in the investigation of the properties of both common and unique fluids. As for rheological studies of the properties of bubble solutions, however, the results are few and far between. In general, studies into the rheology of surfactant and polymer surfactant solutions have mainly been focused on the rheology of foams and bulk solutions rather than single bubbles or films<sup>32-37</sup>. This leads to a shortage of existing data to use in the hopes of relating properties such as shear thinning and viscoelasticity to ideas such as the robustness of spherical bubbles.

Nonetheless, the rheological properties of such solutions were investigated, in the hopes that a correlation could be drawn between characteristics such as shear thinning or viscoelasticity and bubble robustness. This was due in part to the work of Sabadini, Ungarato, and Miranda<sup>3</sup> in which they showed that viscoelasticity alters the behavior and bursting mechanics of bubbles made from surfactant-only solutions. Given the results of that paper, it was hypothesized that the polymeric additives which help to create monstrous free floating bubbles might have some characteristic viscous trait which would explain the mechanism allowing them to reach such impressive sizes. Thus, several solutions

containing popular polymeric additives found on the soap bubble wiki<sup>N4</sup> were created, and their rheological properties examined.

## **2.2 Methods**

### *2.2.1 Sample Preparation*

Several different samples were prepared in order to test a variety of bubble solutions of varying viscosities. Every solution contained Dawn Pro dish soap, as well as water and an active ingredient. The first sample type was a soap and water control, which was a mixture of distilled water and 4% soap by weight. The second was a mixture of 85% glycerol and 4% soap by weight, with the remainder of the solution being distilled water. Two solutions with polymeric additives were made as well. One of the polymers was guar, a common food additive used as a thickening agent which is also a favorite of bubble enthusiasts<sup>N4</sup>. This solution was prepared by mixing powdered guar with ethanol to form a slurry, then adding distilled water and mixing overnight at 50°C, making a stock solution. The stock solution was then mixed with 4% soap by weight and distilled water in order to achieve a range of guar concentrations from 1.50 g/L to 6.00 g/L. The final solution type contained the polymer polyethylene oxide (PEO), which is the active ingredient in commercially available Jlube powder, a common lubricant. The Jlube powder has unknown polydispersity and unspecified molecular weight, and is 25% PEO by weight. These commercial PEO solutions were made by mixing various masses of this powder with distilled water and mixing at room temperature for 30 minutes, at which point soap was added at the same 4% by weight concentration. Concentrations from 0.05g/L to 10.00g/L were created and used for these measurements.

### 2.2.2 Rheological Methods

In order to examine the viscous characteristics of these solutions, every sample was run through an AR2000 rheometer manufactured by TA Instruments. An upper geometry with a 60mm diameter and a 500 $\mu$ m gap height was used for each sample, with trials run at 20°C, 25°C, and 30°C. Once the gap between the upper geometry and Peltier plate was filled with solution, a procedure consisting of a pre-shearing step, an oscillatory step, a second pre-shearing step, and a flow step was run. The two pre-shearing steps were used to remove any memory, if present, from the fluids and return them to equilibrium. For these steps, the sample was sheared at a frequency of 50s<sup>-1</sup> for 10 seconds, and allowed to sit for 1 minute to attain equilibrium. During the oscillatory step, the samples were subjected to oscillatory torques ranging from 0.1 to 1000 $\mu$ N\*m and their storage and loss moduli were recorded. In the flow step, the samples were subjected to shear flow at rates ranging from 10 to 1000s<sup>-1</sup> and their viscosities were recorded.

It can be seen that a valid range of shear rates was examined by means of a simple approximation. Assuming that a bubble solution is pulled away from a string of radius  $r$  at some velocity  $v$  and that the fluid reaches this velocity in a distance approximately equal to  $2r$ , the shear rate is easy to estimate. Using the fact that shear rate is velocity divided by gap width (in this case  $\frac{v}{2r}$ ) it was estimated that a rope with a radius of 5mm moving at 2m/s would provide a shear rate of 200s<sup>-1</sup>. For a more common rope radius of 2mm, moving at the same velocity of 2m/s, the shear rate would be approximately 500s<sup>-1</sup>. Allowing for thinner ropes or higher pulling velocities, it was decided that a max shear rate of 1000s<sup>-1</sup> would serve as a reasonable upper bound for these shear flow experiments. It should be noted that if the bubble solutions do in fact experience Poiseuille-type flow due to

immobile surfactant layers, then the film thickness may be the length scale of interest, rather than the rope radius. Using the same approximations as above, while exchanging the  $2r$  factor for  $\delta$ , the film thickness, it can be shown that a film moving at  $1\text{m/s}$  with a thickness of  $3\text{ microns}$  would experience a shear rate of approximately  $333,000\text{s}^{-1}$ . This rate would be well beyond the range any rheometer could reliably examine. Figure 2.1 below provides a diagram describing this approximation.

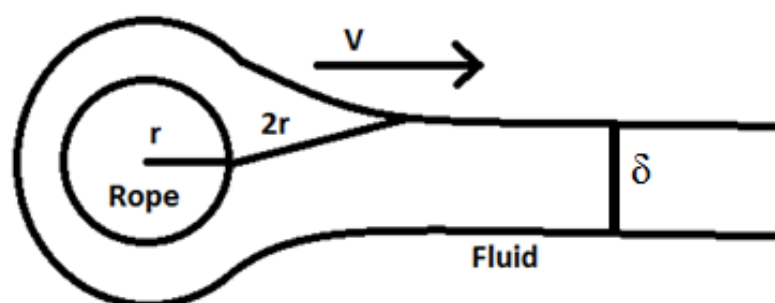


Figure 2.1: Visual approximation of bubble solution being pulled away from a string during film formation. The rope radius is  $r$ , the velocity of the rope relative to the fluid is  $v$ , the film thickness is  $\delta$ , and the distance over which this velocity is achieved is  $2r$ .

## 2.3 Results and Discussion

The viscosity vs. shear rate graphs produced from the shear flow experiments, as shown in Figure 2.2 below, indicate that the solutions containing guar all experience shear thinning, sometimes changing viscosity by an entire order of magnitude over the range of shear rates examined. The control solutions of soap and water and the 85% glycerol solution, however, do not experience any significant shear thinning. The small degree of shear thinning observed for the glycerol solution is likely due to the hygroscopic properties of glycerol, as it very readily absorbs water from the surrounding air (a 10% increase in

mass was measured for pure glycerol left uncovered in the lab over a period of 1 hour). Since a small amount of water added to glycerol can drastically lower its viscosity<sup>38</sup>, this would explain the small change in the solution's shear viscosity during the experiment.

Observing shear thinning in the guar solutions but not in the controls seems to intuitively make sense as it would imply that the solutions containing guar, which make bubbles of impressive size, will experience a shear thinning effect as films form, allowing the solution to expand further than one which retains its viscosity under high shear. Additionally it would imply that after formation, when the shear rates are significantly lower, the bubble film would regain some degree of viscosity, thus making the skin less prone to drainage and therefore more stable. The problem with this conclusion, however, is that the PEO solutions, which make bubbles equally as impressive as the guar solutions, do not exhibit the same shear thinning behavior within the resolution of the rheometer, which renders this line of reasoning ultimately inconclusive.

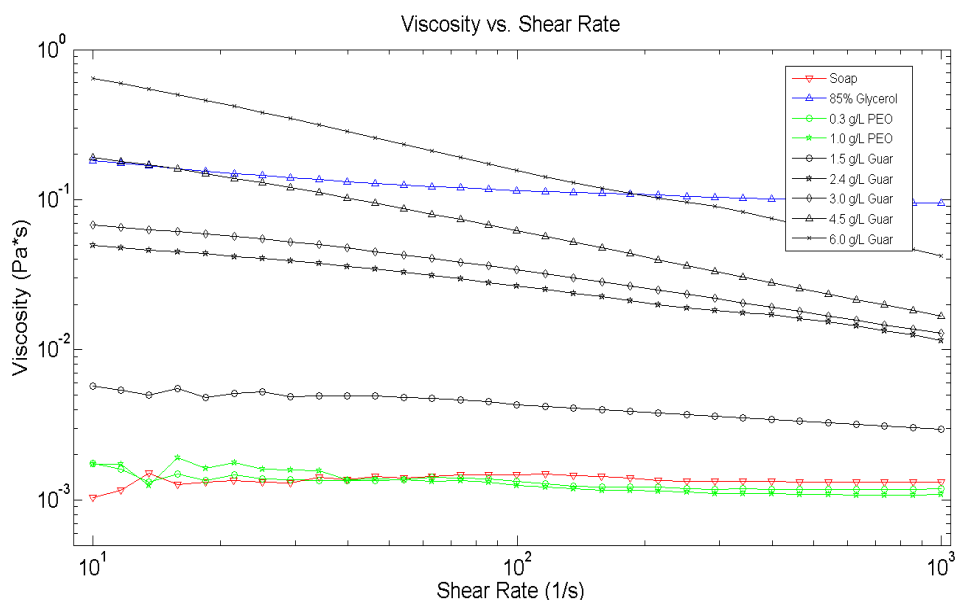


Figure 2.2: Viscosity vs. shear rate graph for control, glycerol, guar, and PEO samples. All guar samples are black, the two PEO samples are green, the glycerol sample is blue, and the control sample is red. All guar samples display at least a small degree of shear thinning over the observed range of shear rates.

## 2.4 Conclusion

While the data taken from these rheological measurements seemed promising initially, it was ultimately determined that no conclusion could be drawn. Shear thinning was shown to not be the mechanism behind enhanced film and bubble formation. This conclusion did lead to a new line of investigation, namely extensional rheology and bursting mechanics. The reasoning behind this was that the creation of films and bubbles is more the result of extensional flow rather than shear flow, and therefore this new line of research would likely be more enlightening in the end. Ultimately, while this rheological approach did not fully answer the question, it exposed a new path which would ultimately become more fruitful.

# Chapter 3

## Extensional Flow and Bursting

### Mechanics of Polymer-Surfactant Films

#### 3.1 Introduction

There proved to be more literature on the extensional flow behavior and bursting mechanics of polymer-surfactant films than there was pertaining to the rheology of their associated bubbles. In the area of extensional flow, several researchers have examined the manner in which the viscoelastic properties of such solutions affect their extension and break-up properties. These works largely come to the consensus that polymeric additives entangle in the solution and enhance “necking”, or extension without rupture<sup>39-42</sup>. Thus, the extensional properties of the solutions in question for this study were investigated to determine the existence of any relationship between fluid extensional properties and bubble behavior.

There also exists a fair amount of research literature on the subject of film rupture and lifetime, if not bubble behavior in particular. Works examining the relationship between viscoelastic characteristics of fluids and their bursting speeds indicate that certain types of surfactants, which form worm-like micelles, increase the rate of film rupture, as they make it so that surface tension is not the only contributing factor in the process due to increased viscoelasticity<sup>3</sup>. Additionally, several research groups have examined bubble lifetimes and the manner in which brittle films retract in the hopes of developing a

predictive model of film lifetimes, with the goal being to gain a better understanding of aerosol dispersion<sup>30, 43-46</sup>. Most of these predictions, however, are geared towards bubbles formed in liquid baths, rather than those floating in air or sitting on a solid substrate, due to increased ease of observation. These works agree in general that large bubbles have longer lifetimes than small bubbles<sup>30, 44</sup> and that rupture characteristics are greatly influenced by gravitational and capillary related drainage<sup>3, 44-46</sup>. This agreement lent credibility to the idea that examining the bursting behavior, as well as the extensional properties, of each fluid may indicate some relation between the solutions' viscoelastic properties and their ability to make larger, more stable films.

## **3.2 Methods**

### *3.2.1 Extensional Flow*

In order to determine the extensional characteristics of each of the samples, each solution was placed in a 25mL glass pipet and the pipet was adjusted so that one drop fell from the pipet every 3-5 seconds. The drips were recorded in high definition (1280x800p) at 1000 frames per second with a Phantom high speed camera from Vision Research. The motion of each droplet was recorded from its formation until the droplet pinched off and disconnected from the fluid in the pipette, as shown below in Figure 3.1. In the event that the droplet did not pinch off before exiting the camera's field of view, the length of the tail visible on camera was recorded instead.

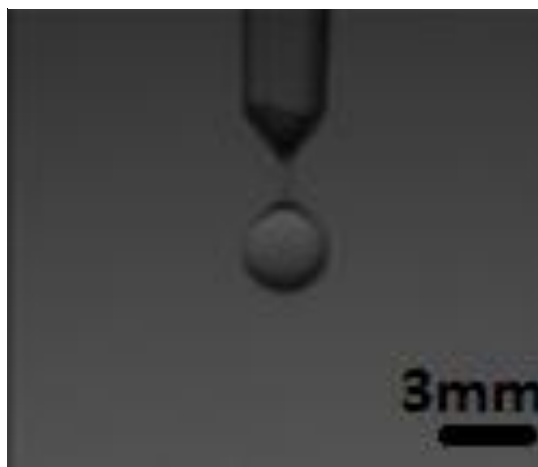


Figure 3.1: Example photograph of a hanging droplet just prior to its tail pinching off.

The length of the tail connecting each droplet to the pipet was measured one frame before the tail could be seen breaking using ImageJ image analysis software. In the event that the tail did not break before the droplet left the frame, the length of the tail that was visible on the screen was measured instead. Additionally, a high resolution photograph was taken of a hanging droplet of each sample. These photographs were used in a program created by Burton *et al.* which computes the surface tension of an axisymmetric hanging droplet<sup>47</sup>, and the surface tension values were recorded.

### 3.2.2 *Bursting Mechanics*

In order to observe the burst behavior of these bubbles, a setup similar to that found in reference 3 was used. The authors of that paper used a clear acrylic enclosure in order to measure the bursting velocity of bubbles made of a surfactant solution at its critical micellar concentration. For this experiment in particular, a clear acrylic cube with a side length of 15cm and a removable top, as shown in Figure 3.2 below, was made to hold the bubbles. A circular platform with a diameter of 10cm and a small hole in the center was glued into the bottom of the enclosure. This platform allowed water to be placed in the

bottom of the enclosure and air to be pumped into solutions placed over the small center hole. The water in the bottom made the enclosure a humid environment, an important factor for bubble stability. Additionally, two wires were soldered to metal contacts which were attached to the wall of the enclosure, allowing the wires to be connected to a power source.

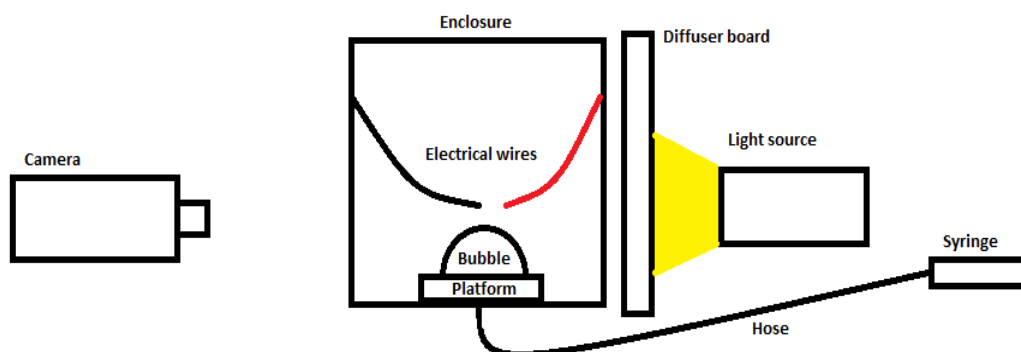


Figure 3.2: Diagram of the apparatus used in the film rupture experiments. The camera recorded footage from one side of the enclosure, and a high power light was placed on the other side of the enclosure behind a diffuser to facilitate better image contrast.

In order to form and observe the bubbles, 500 $\mu$ L of each solution was placed over the small hole in the platform and 50mL of air was pumped into the solution through a hose attached to a syringe. Four bubbles were blown for each solution, and one each was allowed to sit stationary for 30 seconds, 1 minute, 2 minutes, and 10 minutes. At the appointed times, the bubbles were popped with a 10kV open air spark from the electrical wires mounted in the enclosure, which were attached to a high voltage DC power source. The bubble bursts were recorded with the Phantom high speed camera in high definition (1280x800p) at 7500 frames per second with an exposure time of 130 $\mu$ s, and the velocity of the expansion of the resulting hole was recorded using ImageJ image analysis software, as depicted below in Figure 3.3.

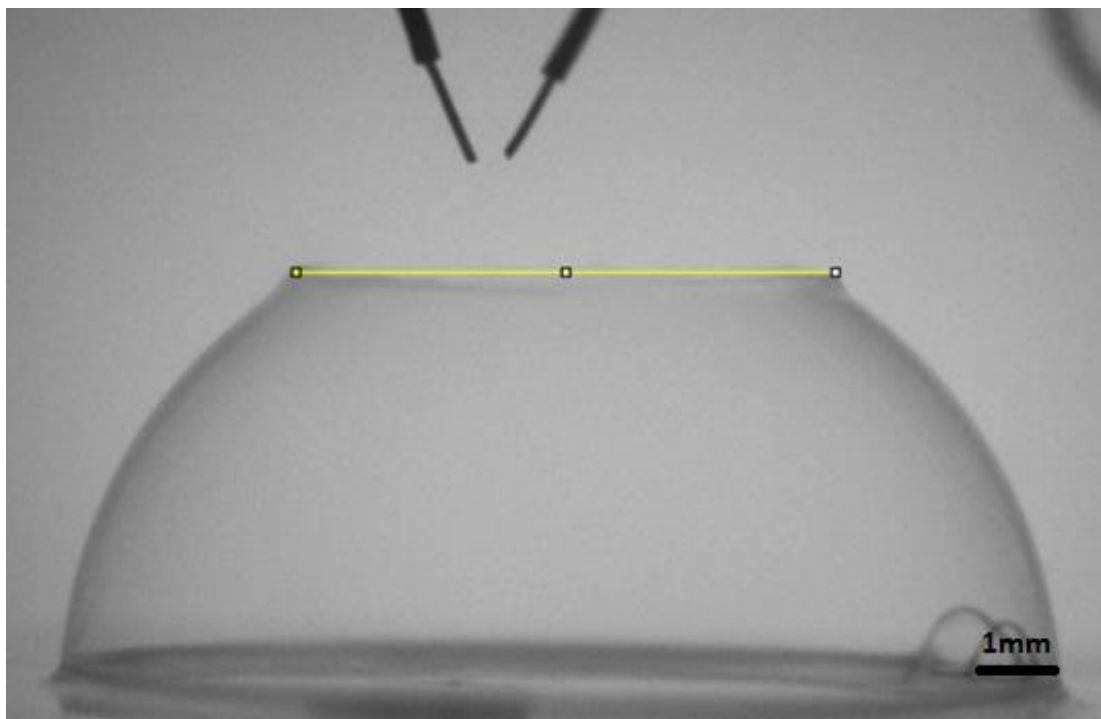


Figure 3.3: Sample screen shot of a frame in which the diameter of a hole in a ruptured bubble was measured. The diameter of the hole was measured every 3 frames for each bubble, for the first 60 frames.

## 3.3 Results and Discussion

### 3.3.1 Extensional Flow Results

The droplet pinch off experiments proved to be fruitful, as they shed light on the relationship between the solutions' extensional properties and their effectiveness in generating more viable bubbles. Some solutions would only extend very slightly before pinch off, while others would seemingly extend indefinitely without pinching off. While the second case sounds like a desirable characteristic when attempting to make a large film or bubble, it can actually prove to be detrimental. It was noticed during the course of these experiments that when the solution didn't pinch off quickly enough, the bubbles formed by that solution either were short lived or fell quickly to the ground and popped. Figure 3.4

below provides screen shots of several different solutions just prior to their pinch off moments.

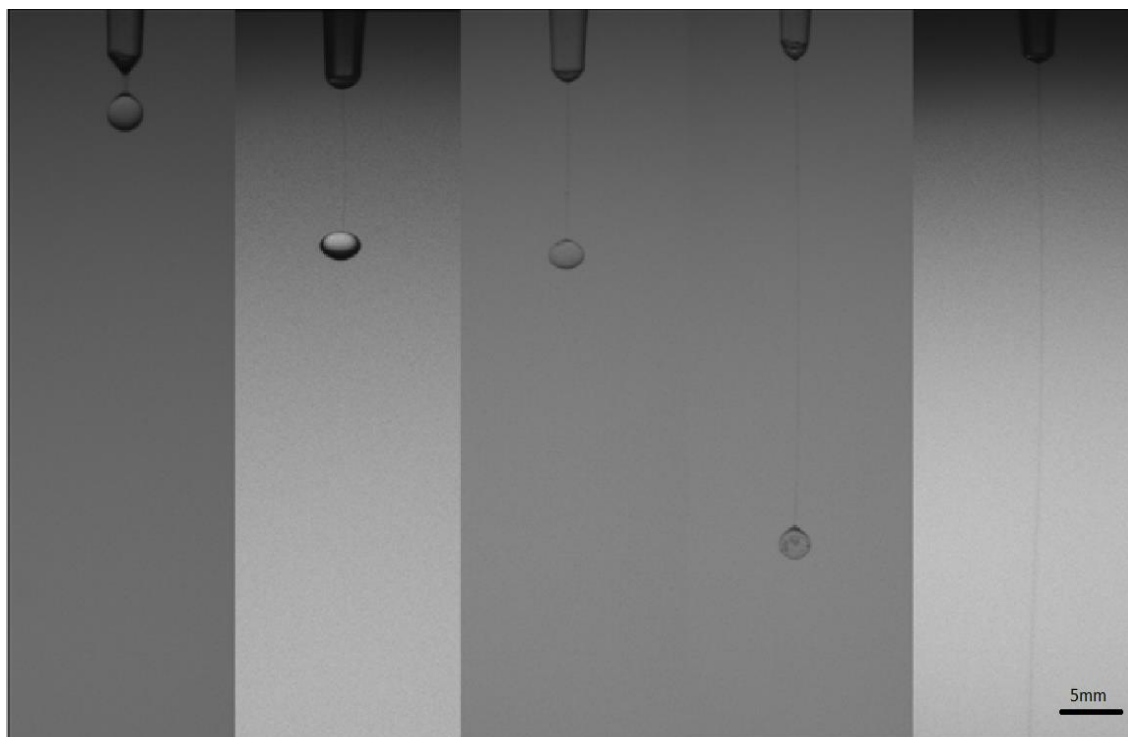


Figure 3.4: From left to right: Soap and water control, 0.3 g/L commercial PEO solution, 2.4 g/L guar solution, 4.5 g/L guar solution, and 1.0g/L PEO solution.

The results of the drop experiments show that even at low concentrations, 0.3 g/L for commercial PEO and 2.4 g/L for guar, the solutions were able to extend an entire order of magnitude further than the soap and water control before rupture, as shown in Table 3.1 below. In fact, the two concentrations mentioned above were the concentrations of each polymer which seemed to most consistently produce the largest and most stable free floating films, thus leading them to be referred to as optimal concentrations<sup>N4</sup>.

Table 3.1: List of the maximum length attained by droplets of each solution as well as the surface tension of each solution. Once the PEO samples achieve a certain concentration, there appears to be a discontinuity in the maximum length the tails can reach.

Sample	Rupture Length (mm)	Surface Tension (mN/m)
Soap	1.5	35
85% Glycerol	74.2 (off screen)	31
1.5 g/L Guar	9.4	35
2.4 g/L Guar	22.5	35
3.0 g/L Guar	39.6	32
4.5 g/L Guar	63.7	31
6.0 g/L Guar	43.2	31
0.05 g/L PEO	3.8	30
0.1 g/L PEO	3.9	31
0.3 g/L PEO	22.9	28
0.5 g/L PEO	24.2	31
1.0 g/L PEO	82.5 (off screen)	32
5.0 g/L PEO	85.6 (off screen)	34
10.0 g/L PEO	73.2 (off screen)	30

In the process of examining a wide range of concentrations of both polymer solutions, it was seen that solutions which extended further than the optimal solutions often formed less stable bubbles, or failed to reliably form them at all. The lower concentrations, on the other hand, formed smaller or less stable bubbles. This indicates that the films need to have some viscoelastic properties, but if the solutions are too viscous, they do not favor the formation of larger free floating films.

### *3.3.2 Bursting Mechanics Results*

The final area examined in this experimental approach, the burst and aging mechanics of the bubbles themselves, provided additional interesting information. As shown below in Figure 3.5, while all of the films had approximately the same burst velocity at short times, after 10 minutes there were noticeable differences between films.

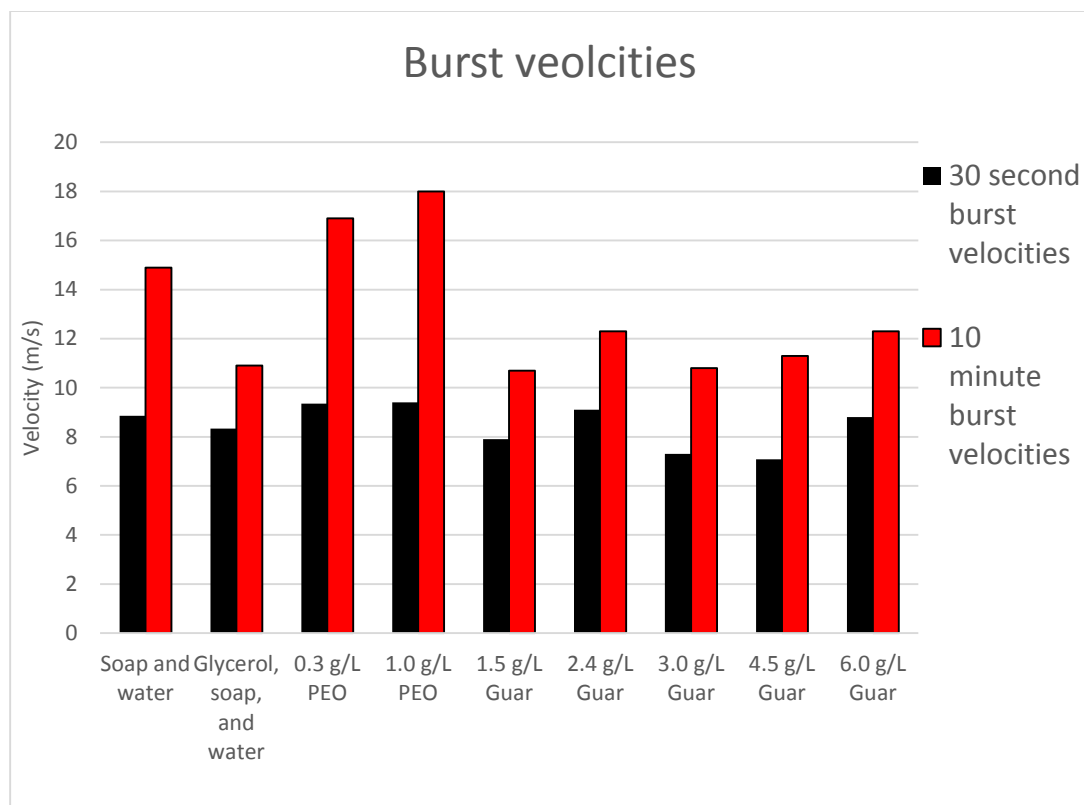


Figure 3.5: Graph depicting the average burst velocities of each sample. The black bars show the burst velocity for all solutions at 30 seconds, while the red bars show the burst velocities for all solutions at 10 minutes. PEO and soap solutions burst significantly faster than the more viscous guar and glycerol solutions.

The more viscous solutions which contained guar and glycerol experienced relatively low burst velocities at the 10 minute time point, while the control and the PEO solutions burst much more quickly. Since the surface tensions and densities of all of the solutions were very similar, with the surface tensions ranging from 28mN/m to 35 mN/m and the densities ranging from 999kg/m<sup>3</sup> to 1006 kg/m<sup>3</sup> (with the exception of the glycerol solution, which had a density of 1218 kg/m<sup>3</sup>), it can be deduced from Eq. 1.1 that the more viscous (see Figure 2.2) films experienced a lesser degree of drainage, leading to higher stability. Also, since the PEO films had higher burst velocities than even the soap and water control, these films either experience a higher degree of drainage or have additional

viscoelastic forces at play, the latter of which may possibly contribute to the ability of these solutions to create massive free floating films<sup>17</sup>.

One other interesting piece of evidence indicating the heightened stability to aging of these films lies in their aging properties in dry environments. In order to examine bubble lifetimes under less favorable conditions, bubbles made from the soap and water control, as well as 2 solutions in the optimal range for guar and commercial PEO each, were made to sit stationary in the acrylic enclosure until rupture occurred. The results for this exercise are shown below in Figure 3.6. All of the observed polymer solutions had longer average lifetimes than the soap and water control. What makes the results interesting is that the guar solutions, which are significantly more viscous than the commercial PEO solutions (nearly 2 orders of magnitude different for the optimal solutions observed), have a shorter average lifetime than the commercial PEO solutions. This supports the idea that there may be factors other than viscosity at play in the commercial PEO solutions which inhibit drainage and increase stability. Further examinations of the films' drainage behavior were used to determine what the factor(s) may be by examining the drainage rate and thickness of the film over time.

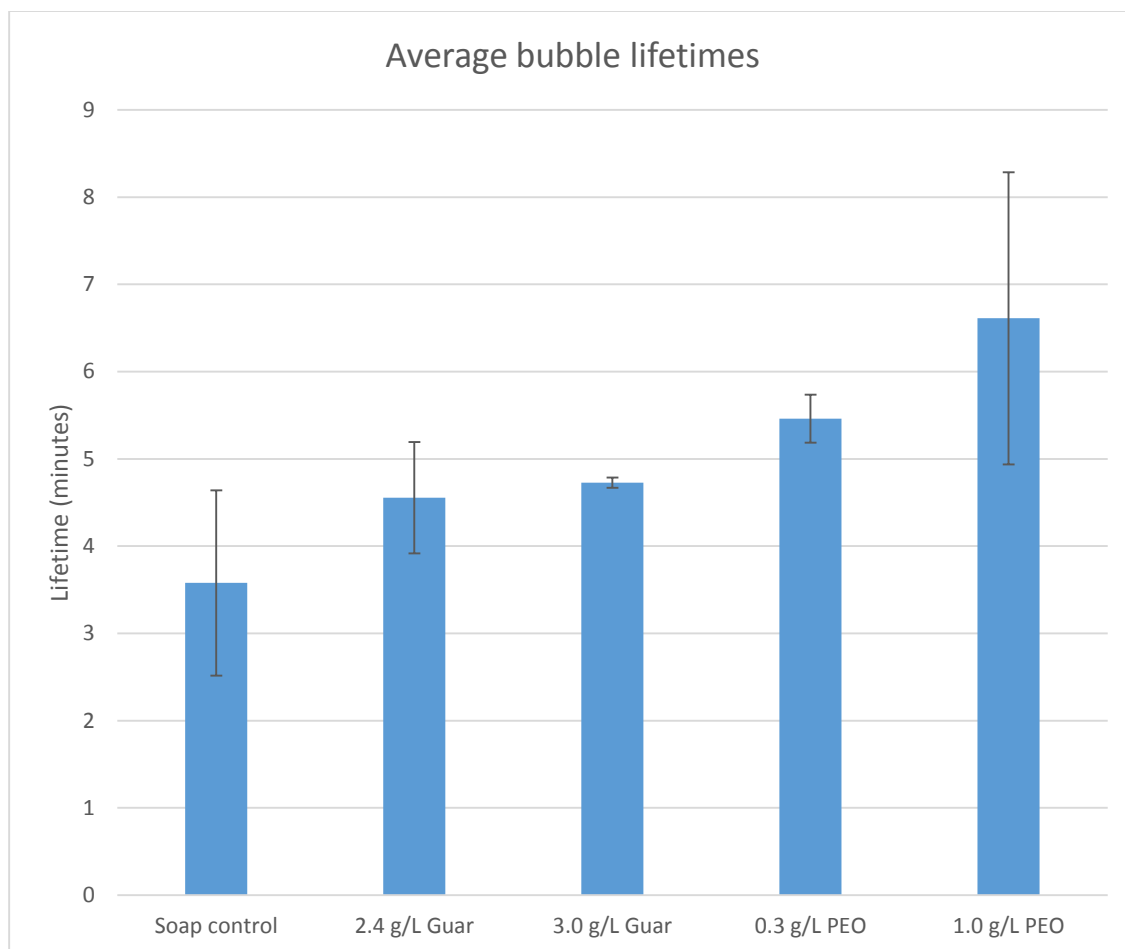


Figure 3.6: Average stationary bubble lifetimes for the soap and water control and optimal guar and commercial PEO concentrations. The less viscous PEO solutions exhibit longer average lifetimes than the more viscous guar solutions. Error bars represent 95% confidence over 3 trials for each solution.

### 3.4 Conclusion

A thorough examination of the extensional and bursting properties of the polymer-surfactant solutions of interest confirmed the idea that the robustness of their associated films is not necessarily related to viscosity or shear thinning capabilities. Additionally, it provided inspiration for the next direction of research, the solutions' drainage properties. This is due to the results of the bursting mechanics studies in particular, as they pointed towards interesting drainage behavior which was independent of the solutions' viscosity.

These results made it apparent that a more in depth examination of the drainage profiles of polymer-surfactant solutions was called for, both with respect to the height along the profile of the films as well as time.

## Chapter 4

# Drainage Profiles of Vertical Polymer-Surfactant Films

### 4.1 Introduction

Since films and foams provide a good model of two dimensional systems as well as their prevalence in industrial processes such as curtain coating, aerosol dispersion, and water treatment, there has been a great push over the last two decades to understand more about film behavior. In particular, many researchers examine the manner in which films and foams drain in the hopes that they may shed light on how to better manage these metastable systems<sup>5-26</sup>. Despite all of the interest in soap film drainage, there are currently no full experimental profiles of a film draining under gravity. Generally, researchers either perform a numerical analysis in order to see if the theory matches with visual observations of film drainage profiles<sup>6, 8, 9</sup>, or experimentally examine the drainage rate at a single point on a small (typically 1mm to 1cm) scale film using interferometry techniques<sup>10, 12, 17, 19, 20</sup>.

One other area commonly examined by researchers is entrainment of soap films. In other words, they examine the thinning properties of films as they are being drawn upwards at some velocity  $Q$ <sup>5, 14-16, 22-26</sup>. This does not offer a full profile of the thickness of the film, but rather a measurement of the thickness at a single height as a function of time for the moving film. A full profile of these films draining under gravity is absent from the literature for both surfactant films and polymer-surfactant films.

Due to this lack of a full drainage profile and to the interesting drainage characteristics previously observed in these films, an experiment was designed which would allow for a full experimental profile of vertical film drainage with respect to both height and time. In the spirit of prior experiments in this thesis, it was decided that the profiles examined would be much larger in size than those found in the literature, approximately 15 cm by 15 cm. This size range was decided upon as it would be more likely to elucidate the drainage and thickness properties of the larger free floating films which inspired this line of research, while still being easily constructed in a lab setting.

## **4.2 Methods**

### *4.2.1 Sample Preparation*

Samples prepared for these experiments were prepared in much the same manner as those in earlier sections, only with fewer solutions. The exact same control, 2.4 g/L guar, and 0.5 g/L commercial PEO solutions as in Chapters 2 and 3 were used here, along with solutions consisting of differing concentrations of sodium dodecyl sulfate (SDS) and 98% pure 2,000,000 g/mol PEO. Specifically, the combinations used were a solution of water and 2% by weight SDS, water with 2% by weight SDS with 0.5g/L PEO, water with 4% by weight SDS and 0.5g/L PEO, and water with 0.5g/L PEO and 4% by weight Dawn Pro dish soap. The solutions consisting of 2% by weight SDS were chosen in order to match with solutions used by experimentalists in the literature, while the solution with 4% SDS was used to imitate the concentration of dawn dish soap in the other solutions examined during the course of this thesis.

#### 4.2.2 Thickness Measurement Methods

In order to properly measure the drainage profiles of these soap films, it was necessary to construct a spectrometer which operated with a long wavelength of light. Much of the inspiration for the design of this apparatus was taken from a paper by Wu *et al.*<sup>7</sup>. The device was constructed using an infrared 3 $\mu\text{m}$  wavelength LED, a photodiode resistor designed to pick up infrared light, and an optical chopper. The wavelength of the light was chosen to allow for the measurement of thicker films while minimizing error, as water has a large absorbance peak at 3 $\mu\text{m}$ , while the photodiode resistor was used since its resistance would change with the amount of infrared light incident upon it. The optical chopper was used in conjunction with a lock-in amplifier in order to reduce noise and focus on a signal recorded at a certain frequency, in this case 600Hz. All of these devices were affixed to an aluminum plate with a hole measuring approximately 27cm by 8cm in it and adjustable posts which allowed the height of the platform to be changed without disassembling the apparatus while measuring film thicknesses. The last component of the spectrometer was a polished aluminum sheet, with a hole for the LED to shine through, placed between the optical chopper and the soap films. This sheet allowed for a strong reduction in reflected and scattered IR light read by the photodiode, as aluminum is a black material in the IR spectrum. The entire apparatus was placed inside a clear acrylic box to block external air currents and allow for humidity control. A picture of the completed device is shown below in Figure 4.1.

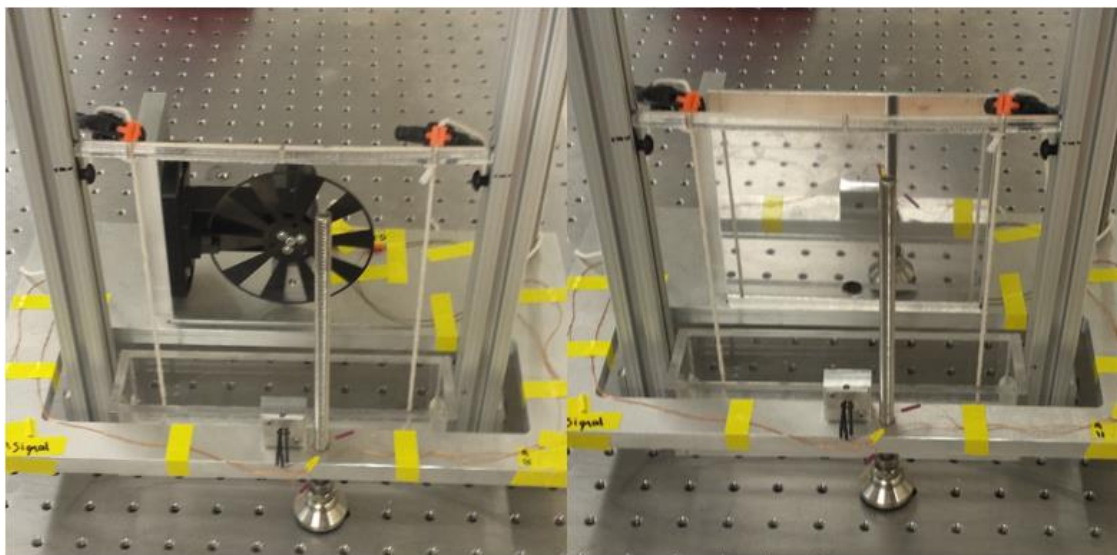


Figure 4.1: (Left) Image of the custom made spectrometer without the aluminum reflective plate in place. The screw post in the image was used to easily adjust the height of the platform, the black fan is the optical chopper, and the metal cubes next to the screw post and behind the chopper are the photodiode resistor and IR LED, respectively. (Right) The same device, with the aluminum reflective plate in place.

Creating the films themselves involved a less complicated setup. A small tub was made out of acrylic and placed between two beams. The beams supported an acrylic bar with two holes in it at a height of 15cm above the top edge of the tub. Cotton strings with thicknesses of approximately 3mm were tied to two loops in the base of the tub so that they would pass vertically upward and through the holes in the acrylic bar, and a final string was tied horizontally from one of the vertical strings to the other, so that it sat just below the horizontal bar. With the strings arranged in this way, a 15cm square film could be created by submerging the strings in the tub when it was filled with solution and pulling them upwards.

Actually recording data required the use of some electronics principles. Using the fact that the photodiode had a built in resistance which changed depending on the amount of infrared light it received, it was fairly straightforward to build a voltage divider in order to measure the output voltage across the circuit, and from that the intensity of the light

received by the diode. A blocking capacitor, as shown below in Figure 4.2, was added to the circuit to make it so that the voltage read by the lock-in amplifier was AC voltage, as the capacitor would “block” any DC readings, thus allowing the amplifier to easily read small fluctuations in the output voltage. The voltage divider circuit lowered the voltage across the photoresistor and allowed for measuring small fluctuations in the output voltage,  $V_{out}$ . It was not possible to estimate  $V_{out}$  given the current setup; it could only be directly measured. This is because estimation would require knowing the incoming intensity of the light and the exact baseline resistance of the photoresistor, the former of which was not measurable with the means available. The lock-in amplifier read the output voltage,  $V_{out}$ , at a rate of 600Hz, the same rate at which the optical chopper blocked the light source. This allowed for significant reduction in signal noise, as the amplifier would not read any signal received by the diode at any different frequency. Figure 4.2 below provides a circuit diagram of the voltage divider.

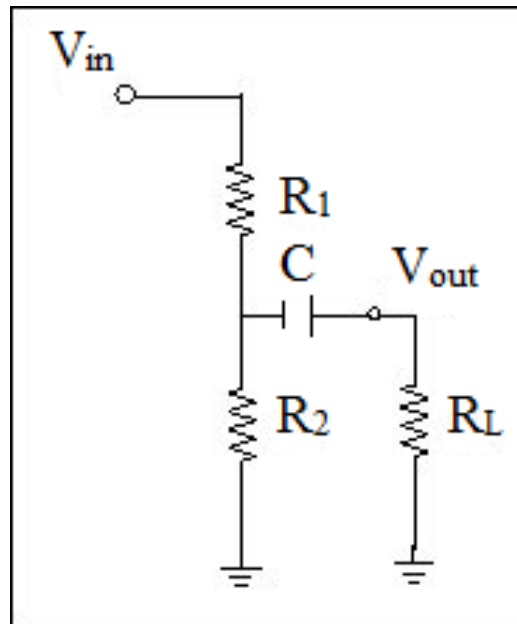


Figure 4.2: A circuit diagram of a voltage divider with a blocking capacitor. In this case,  $V_{in}$  is 18.0 V,  $R_1$  is 1 M $\Omega$ ,  $R_2$  is the voltage of the photodiode resistor (1 M $\Omega$   $\pm$  variations),  $R_L$  is the resistance of the lock-in amplifier (10 M $\Omega$ ),  $C$  is 20  $\mu$ F, and  $V_{out}$  is measured by the lock-in amplifier.

When taking measurements of the film thicknesses, the acrylic tub was filled to the top with the desired solution, and the string was submerged in the bath. Then, with the spectrometer running and feeding measurements into the lock-in amplifier, the string square was pulled steadily upwards over a period of approximately one second and affixed to the support beams so that the film could steadily drain without being disturbed and the top could be placed on the acrylic container around the spectrometer. This process was carried out 5 times at each desired height of the film. The heights ranged from 12.7mm to 139.7mm in 12.7mm increments (0.5 inches to 5.5 inches in half-inch increments), for a total of eleven observed heights and 55 total trials for each type of solution.

The signal read by the lock-in amplifier was averaged every 300ms and fed into LabVIEW, a commercially used laboratory measurement software. LabVIEW then generated a plot of voltage with respect to time, in which the output voltage was measured once every second or once every 500ms, depending on the typical lifetime of the films being observed. A future goal of these experiments will be to find reliable methods of shortening the signal averaging times without a significant increase in noise.

For every solution type, the raw data read from the spectrometer was a graph of voltage vs. time. The voltage readings were converted into thickness measurements using the fact that the voltage read across the photodiode is directly proportional to the intensity of the light incident to it. Thus, the equation

$$\frac{I_T}{I_0} = \frac{(1-R)^2 e^{-\frac{2h}{z_0}}}{1-R^2 e^{-\frac{2h}{z_0}}}, \quad (\text{Eq. 4.1})$$

in which  $I_T$  is the transmitted light intensity,  $I_0$  is the incident light intensity,  $z_0$  is the extinction length of  $3\mu\text{m}$  light in water,  $h$  is the thickness, and  $R = \frac{(n-1)^2}{(n+1)^2}$  is the reflectance<sup>7</sup>, can be altered into

$$\frac{V_{out}}{V_i} = \frac{(1-R)^2 e^{\frac{-h}{z_0}}}{1-R^2 e^{\frac{-2h}{z_0}}} \quad (\text{Eq. 4.2})$$

Using the further approximations that  $z_0 = 0.9\mu\text{m}$  and that  $n = 1.17$  implies that  $R = 0.61\%$  for these solutions as done by Wu *et al.*<sup>7</sup>, this equation can be reduced to

$$V_{out} = V_i e^{\frac{-h}{z_0}} \quad (\text{Eq. 4.3})$$

In this case,  $V_i$  is the initial baseline voltage read across the photodiode prior to blocking the beam with the film and  $V_{out}$  is the voltage read across the photodiode while a film was blocked. These approximations proved to be very useful in determining the thickness of the films, as it reduced the problem to solving Eq. 4.3 for  $h$  and plugging in the measured values of  $V_i$  and  $V_{out}$ .

### 4.3 Results and Discussion

The measurements of the films' thicknesses provided by the spectrometer contained a wealth of information. The initial raw data, as depicted below in Figure 4.3, indicated a high degree of repeatability for the drainage rates of several of the polymer surfactant solutions, and even for the soap and water control.

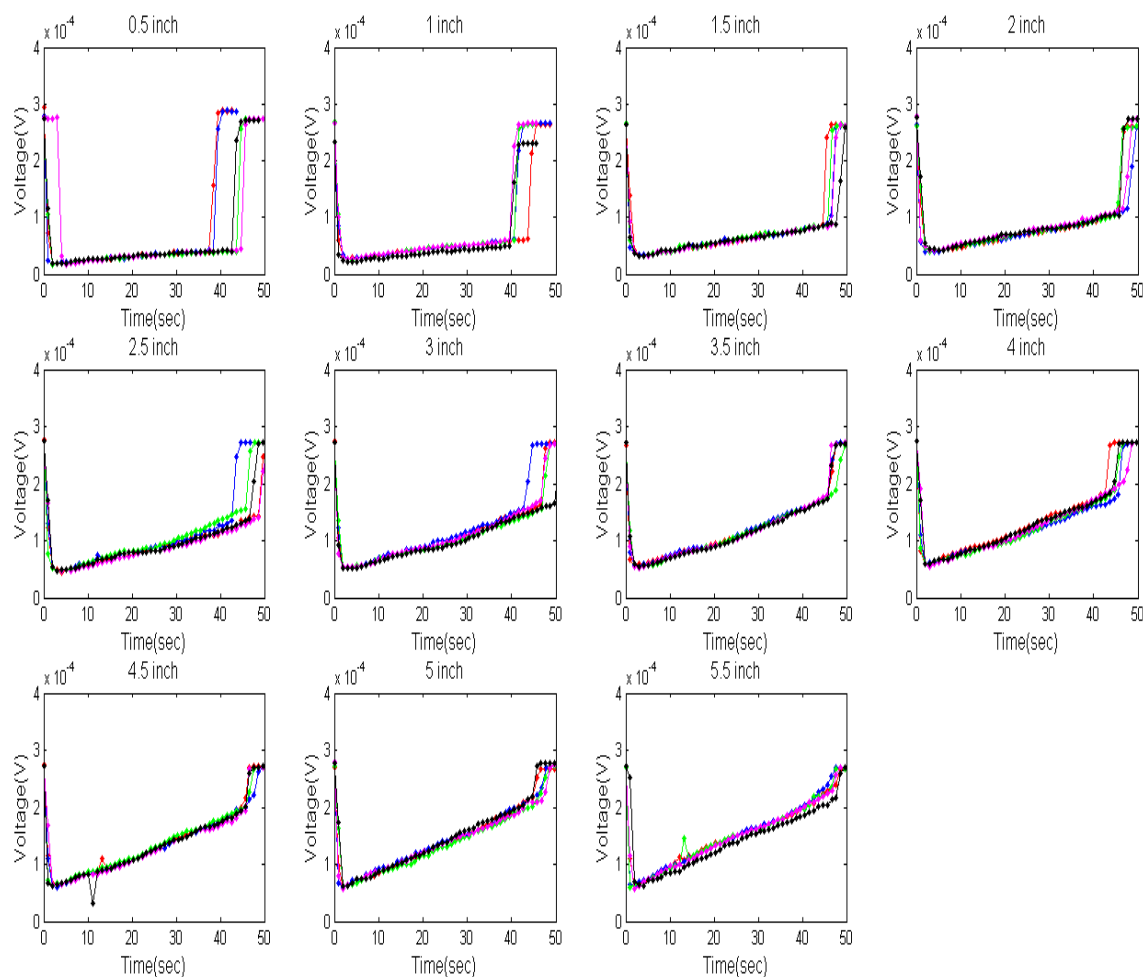


Figure 4.3: Set of graphs depicting the change in voltage with respect to time for all heights and trials using the 0.5 g/L PEO and 4% by weight soap solution. As can be seen qualitatively from the pictures, the drainage rate gradually increased with height. The initial and final voltage jumps correspond with the times at which the films first blocked the IR beam and when they popped, respectively.

As can also be seen in Figure 4.3, not all films ruptured at the same time. Due to this unavoidable circumstance, for each trial height, the data depicting the voltage change was kept and averaged with the other data at each corresponding time point over the shortest film lifetime at the given height. For example, if the five trials run at the half inch height for this PEO and soap solution lasted 25, 37, 30, 32, and 36 seconds each, then the data from each trial running up to 25 seconds were kept and averaged together at each time

point. Figure 4.4 depicts the data after being normalized to have every trial run the same amount of time.

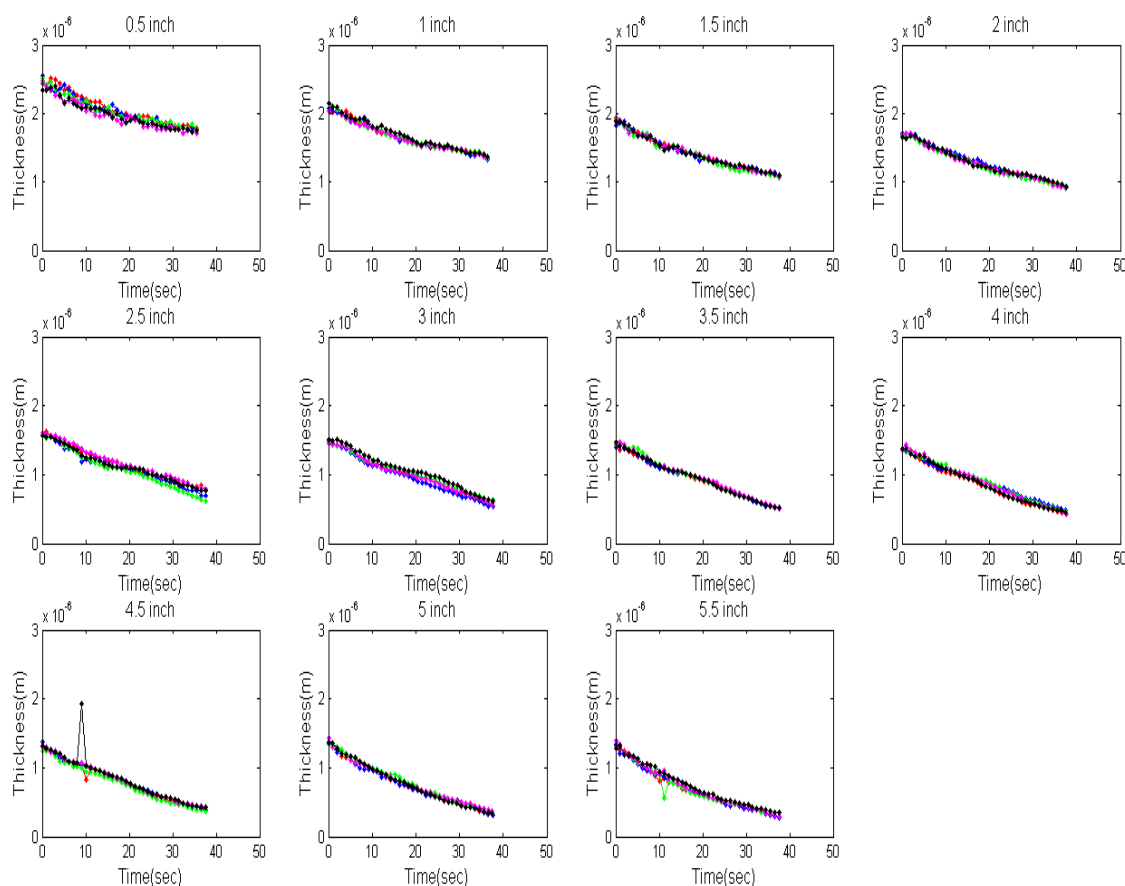


Figure 4.4: Set of figures showing the normalized thickness vs. time data from Figure 4.3 after Eq. 4.3 was applied to it. For each of the 11 heights, the average thickness values were calculated at each time, and a linear fit was applied to the resulting set of points.

Fitting a least-squares line through the averaged data points which resulted from the data as exhibited in Figure 4.4 provided the average drainage rate for each solution at each height. Future experiments with these films will seek to examine whether these films do in fact drain at a linear rate, or whether there is a different type of time dependence exhibited in their drainage with respect to time.

Additional calculations carried out on these data provided measurements of average film lifetime as well as average initial film thickness. The average film lifetime, as depicted

below in Figure 4.5, is greatly altered depending on the combination of polymer and surfactant in the given solution. Interestingly, the combination of 4% by weight SDS and 0.5 g/L of pure PEO had the shortest average lifetime of  $1.80 \pm 0.28$  seconds (95% confidence), while the 4% by weight soap with 0.5 g/L pure PEO solution had the longest average lifetime at  $37.44 \pm 0.10$  seconds (95% confidence). For all solutions in which SDS was the active surfactant, the average lifetimes were markedly short and the addition of a polymer had little to no effect. In every case where polymeric additives were put into a solution with soap and water however, the average bubble lifetime was demonstrably long, often two to three times as long as for SDS solutions. This lends credence to the idea that while SDS may be a common and well researched surfactant, it is not as effective as typical soap in the formation of large films.

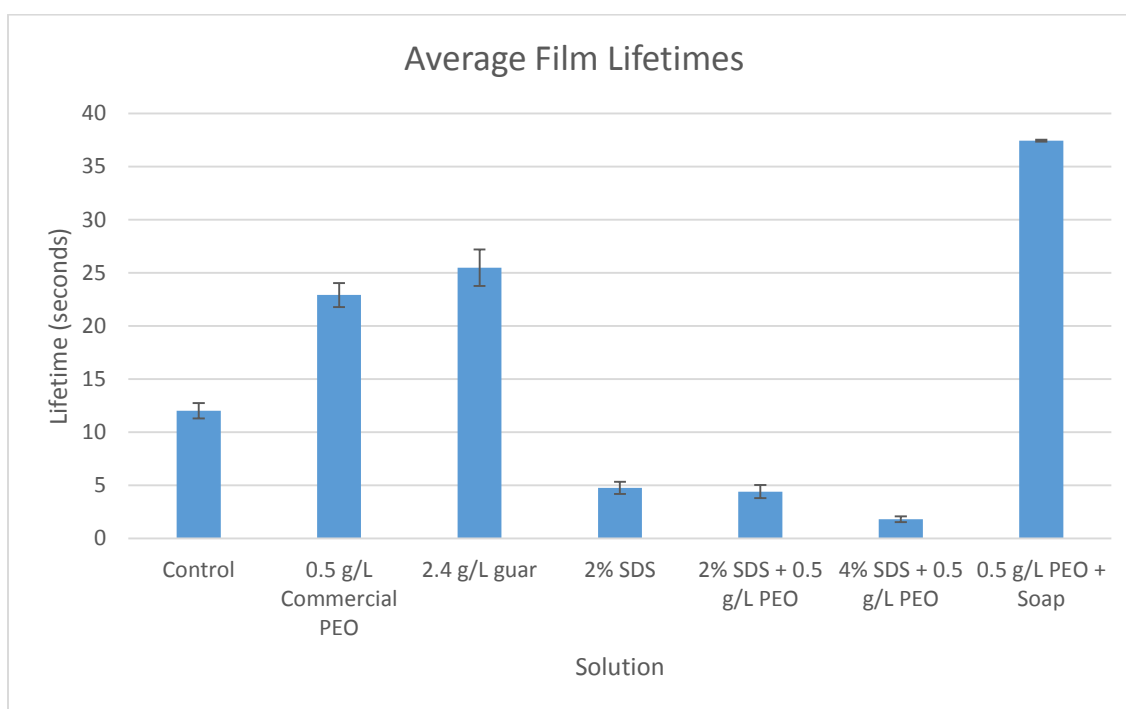


Figure 4.5: Chart depicting the average lifetime for films made by each solution. The four longest lived solutions all have dish soap as their active surfactant, while the shortest lived solutions contain varying amounts of SDS. Average lifetimes were calculated over all 55 trials for each solution, and error bars represent 95% confidence.

While it was hoped that a significant difference would also be seen between the thicknesses of polymer surfactant films and surfactant only solutions, this proved to not be the case. Figure 4.6 below shows the average starting initial thickness profiles for each film type, with error bars to 95% confidence.

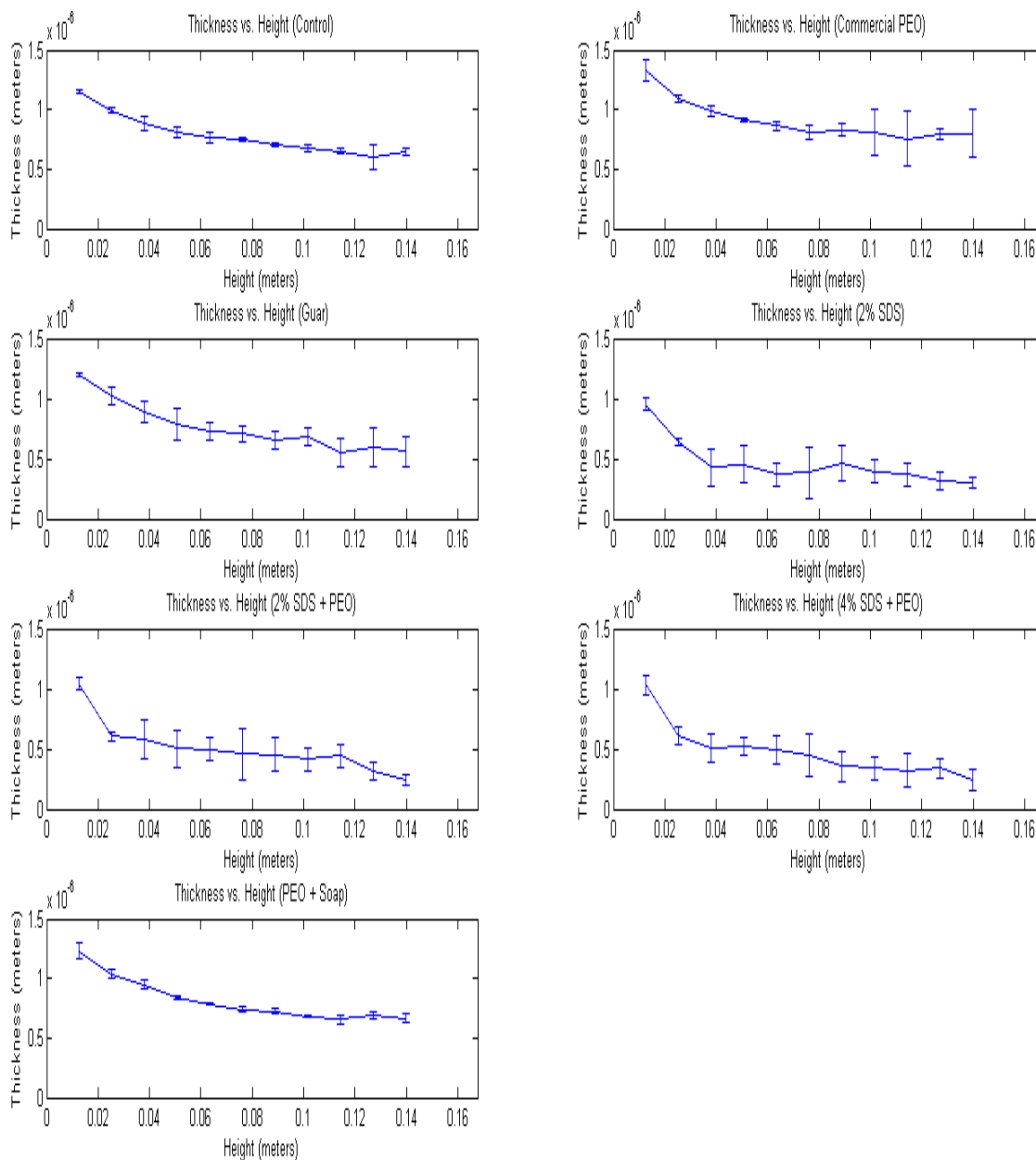


Figure 4.6: Separate initial thickness profiles for each type of solution, with error bars denoting 95% confidence. As the graphs show, there is no significant difference between initial thicknesses when polymers are added to the solutions, either for soap solutions of SDS solutions. Vertical height was plotted on the x axis for ease of viewing.

This lack of significant difference becomes more apparent when the solutions consisting of the same surfactant but different polymer concentrations are all placed on the same graph, as shown in Figures 4.7 and 4.8 below.

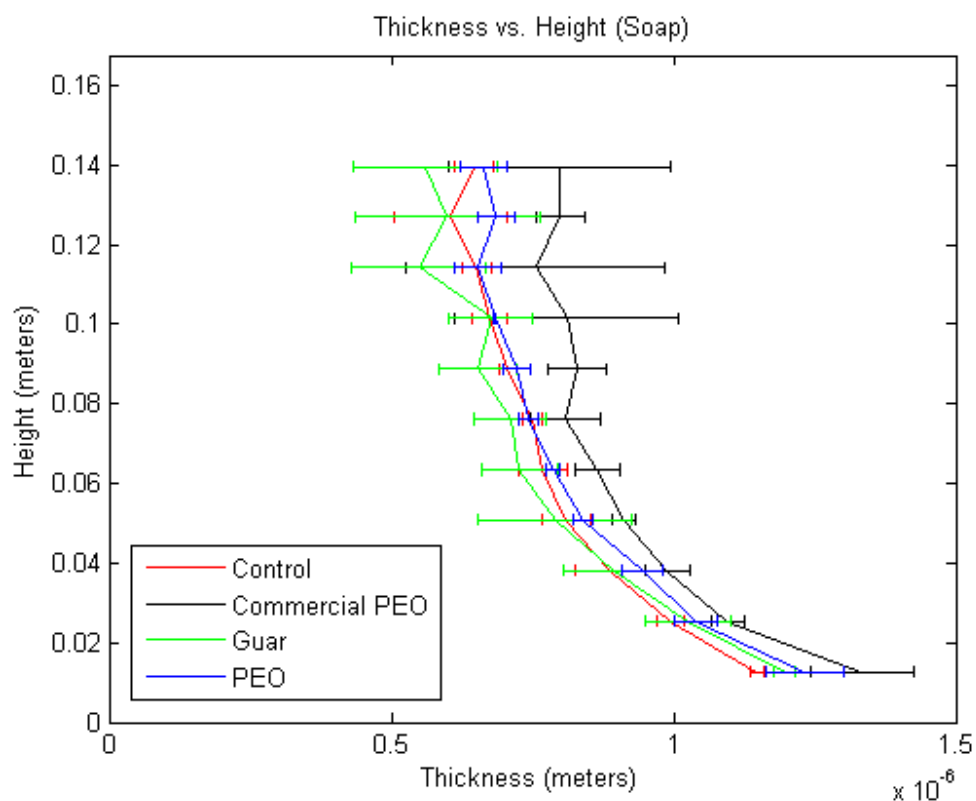


Figure 4.7: Graph depicting the thickness as a function of height for all solutions with soap as the active surfactant. While the solutions containing polymers may be slightly thicker, the difference is not significant compared to the error from the instrument.

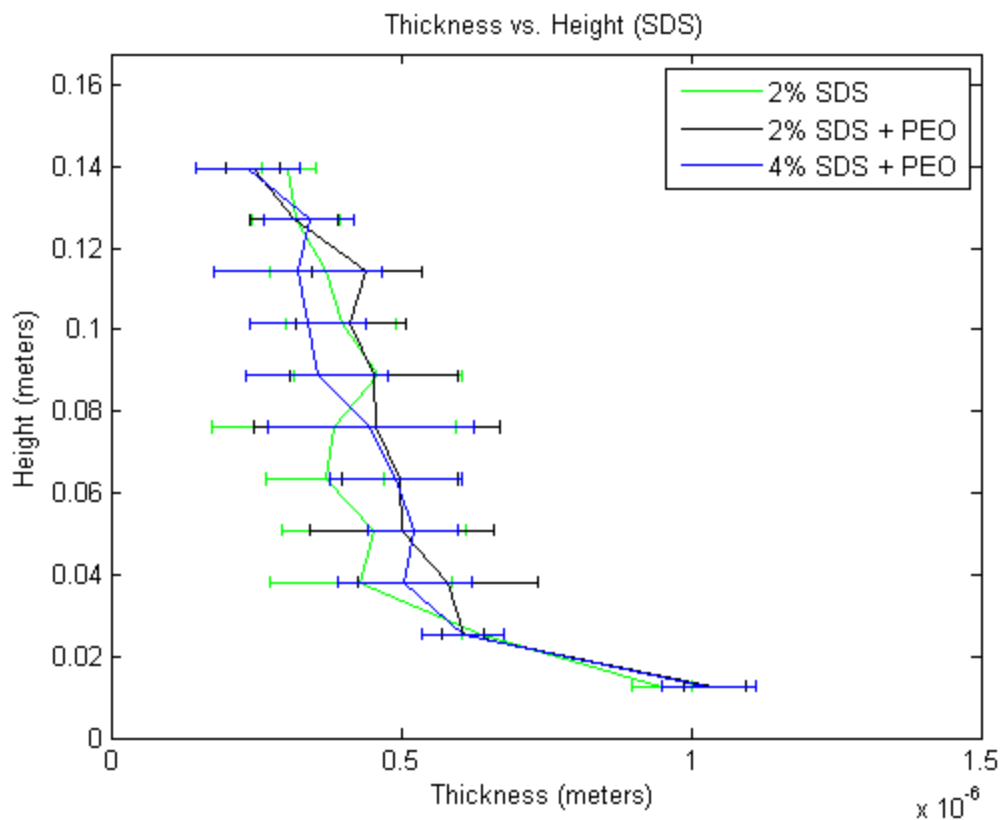


Figure 4.8: Graph depicting the thickness as a function of height for all solutions with SDS as the active surfactant. As above, the solutions containing polymers may be slightly thicker, but the difference is not significant compared to the error from the instrument.

As the two graphs above show, there is nothing to indicate that polymeric additives make a solution thicker initially. That is not to say, however, that they do not affect the thickness over time; in fact, that is what makes these solutions so unique. Figure 4.9 below helps to illustrate this point. When the thickness with respect to time of each polymer-soap solution at the highest measured point (139.7mm or 5.5 inches) is plotted on the same graph, it becomes apparent that these solutions do in fact drain more slowly on average than the soap and water control. This is extremely important for the formation of large bubbles, as the more slowly a bubble drains, the longer it lives in general.

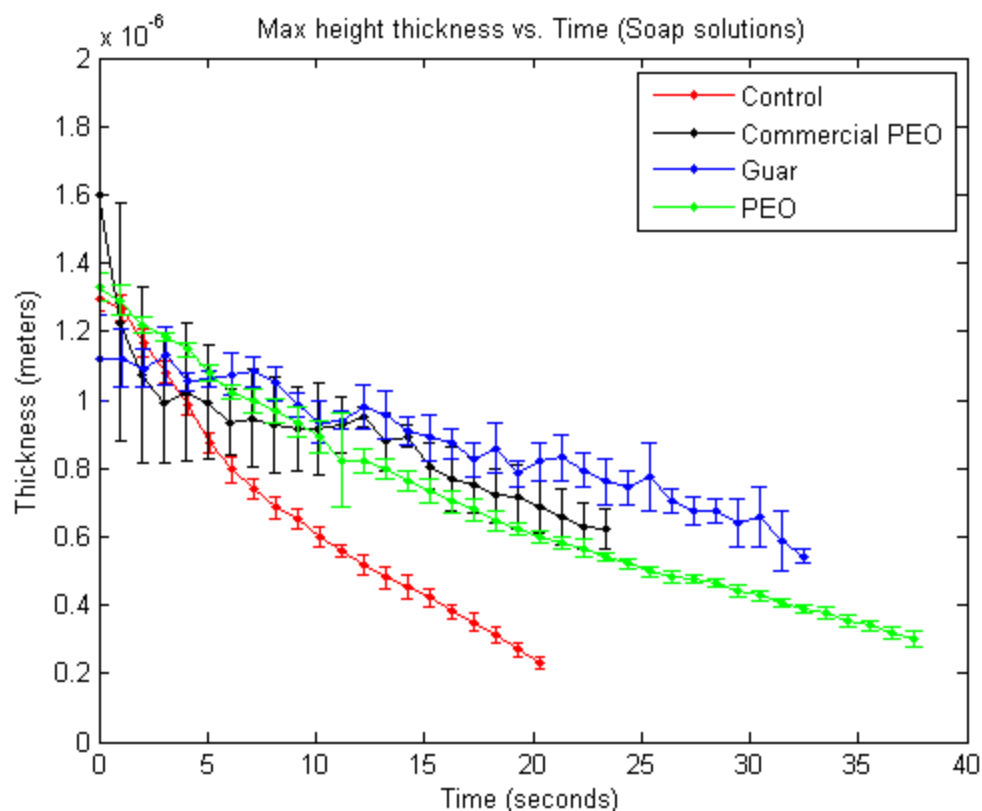


Figure 4.9: Graph of thickness vs. time for each polymer-soap solution at the maximum measured height. The soap and water solution (red) clearly drains much more quickly than the solutions containing soap and polymers. Error bars represent 95% confidence, and are obtained from the average of 5 measurements at each time point.

It can also be shown that the longer average film lifetimes correspond to longer average bubble lifetimes. As can be seen below in Figure 4.10, there seems to be a good correlation between the average lifetime of bubbles and films made from the same solution. Thus, if a vertical film made from a solution is short lived, then a bubble made from the same solution will be short lived. Likewise, if a film has a long lifetime, then a bubble from the associated solution will as well. More steps need to be taken to better quantify the relationship between bubble and film lifetimes, but these initial results show that film behavior can be a suitable proxy for predicting the lifetime and robustness of bubbles.

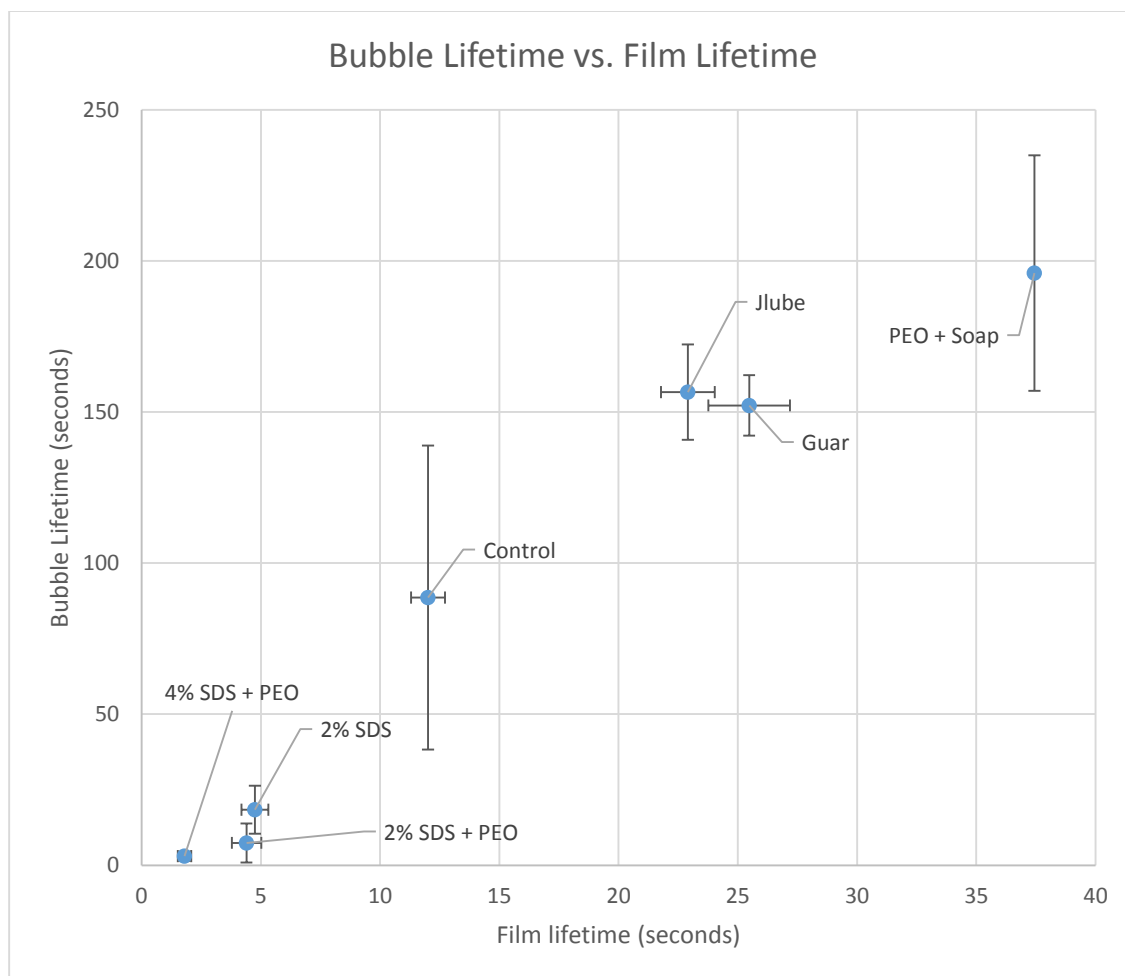


Figure 4.10: Graph depicting the average bubble lifetime vs. average film lifetime for each solution. There is a good correlation between film lifetime and bubble lifetime, so the more robust a film of one solution is, the more robust its bubbles will be. The horizontal error bars represent 95% confidence over 55 trials, the vertical error bars represent 95% confidence over 5 trials.

## 4.4 Conclusion

The results of this line of research provided clear evidence as to how these solutions are able to create giant bubbles. It is easy to see from these data that polymeric additives in conjunction with certain types of surfactants do in fact have a pronounced effect on the drainage behavior of thin films. This is in strong agreement with the results seen when examining the extensional and bursting characteristics of the solutions, as well as assertions made by authors in the literature<sup>22</sup>. In short, these data show that film lifetime is greatly

increased and drainage is greatly reduced by the addition of polymers to soap solutions. These results also show that the longer lifetimes observed for vertical films do, in fact, translate over to spherical films. These traits, along with favorable surfactants and the enhanced necking abilities given to the solutions by the addition of polymers<sup>39-42</sup>, allow for the formation of truly massive bubbles.

# Chapter 5

## Summary

### **5.1 Effects of polymeric additives on the drainage behaviors of soap films**

During the course of this thesis research, attempts to answer single questions have often led to many more questions arising. The task of answering these questions has proven to be challenging yet rewarding. Each new question which has been raised has led to further enlightenment as to the behavior of these films which can create uniquely beautiful, massive bubbles.

While investigating the rheology of polymer surfactant solutions, it was discovered that solutions with wildly different viscosities and shear behaviors could produce similarly impressive free floating films. This was contrary to initial expectations, as it was predicted that there would be a strong relation between the shear behavior of the solutions and their ability to create films. This did, however, open up a new line of inquiry, namely an investigation into the behavior of these films when subjected to extensional flow as well as an examination of the mechanics of these bubbles when bursting.

The results of the extensional and bursting experiments were very useful, as they indicated a strong relationship between the drainage properties of these films and their overall robustness. It was shown that the concentration of polymers had a profound effect on both droplet pinch off length and bubble rupture velocity. At concentrations found to be optimal both from direct observation and assent of the online community<sup>N4</sup>, solutions were

found to have similar extensional characteristics, yet strikingly different burst velocities. This indicated the importance of drainage when considering the robustness of films and bubbles made from these solutions. This observation was corroborated by the results showing longer lifetimes for stationary polymeric spherical bubbles as compared to surfactant-only bubbles. With this evidence in mind, the investigation moved towards the drainage and thickness of the films in question.

The experiments measuring the drainage of vertical soap films proved to be the most significant, as they confirmed the idea that polymeric additives create longer lived, more robust bubbles and films, especially at larger sizes. It was seen that on average, soap films mixed with polymers such as guar and PEO experience average lifetimes which are 2-3 times longer than those of simple soap and water solutions, a result which carries over to spherical bubbles as well. More importantly, it was shown that these solutions also drain at a slower rate. These factors, coupled with the enhanced extensional abilities imparted to solutions by the addition of polymers, provide the necessary recipe for truly impressive bubbles.

These experiments also leave room for further investigations into the drainage behavior of these films, as continued refinement of the experimental methods may lead to a full film profile with respect to time as well as height, something that is currently unseen in the literature. The data from these measurements have shown that certain types of polymer surfactant combinations have higher initial thicknesses. This invites further research, as determining the types of combinations which are most effective at forming thick, robust films is useful not only from the standpoint of a bubble enthusiast, but also to those who may wish to improve or refine industrial processes which depend upon these

polymer-surfactant films. In this same line of reasoning, it has been observed that the 98% pure, 2 million molecular weight PEO from Aldrich provides much longer lived and more stable films than the commercially used PEO of uncertain polydispersity and molecular weight. Thus, it would be useful in future research to determine if there is any relationship between the molecular weight or purity of polymer additives and the resulting robustness of their associated films.

Ultimately, this thesis research has shown that polymer additives in surfactant solutions greatly increase the lifetime and decrease the rate of drainage of both vertically fixed and free floating films. Additionally, it has shown that different types of polymers may have wildly different bulk effects yet solutions of each polymer may have similar behavior when stretched into thin films and bubbles. This work has also opened the door for further research in this lab into the effects of polymer additives on the thickness of free standing films over time, as the current experimental setup provides a means of investigating exactly that characteristic. With good fortune and thorough investigation, this work could lead to a full experimental profile of the drainage of these films as a function of both time and height, something yet to be seen in research.

# Bibliography

- (1) Lautrup, Benny. *Physics of Continuous Matter: Exotic and Everyday Phenomena in the Macroscopic World*. 2nd ed. Boca Raton: Taylor & Francis, 2011.
- (2) Witten, Thomas A., and Philip A. Pincus. *Structured Fluids: Polymers, Colloids, Surfactants*. Oxford: Oxford University Press, 2010.
- (3) Sabadini, Edvaldo, Rafael F. S. Ungarato, and Paulo B. Miranda. "The Elasticity of Soap Bubbles Containing Wormlike Micelles." *Langmuir* 30, no. 3 (2014): 727-32.
- (4) Bird, James C., Riëlle De Ruiter, Laurent Courbin, and Howard A. Stone. "Daughter Bubble Cascades Produced by Folding of Ruptured Thin Films." *Nature* 465, no. 7299 (2010): 759-62.
- (5) Lal, Jyotsana, and Jean-Marc Di Meglio. "Formation of Soap Films from Insoluble Surfactants." *Journal of Colloid and Interface Science* 164, no. 2 (1994): 506-09.
- (6) Van Nierop, Ernst A., Benoit Scheid, and Howard A. Stone. "On the Thickness of Soap Films: An Alternative to Frankel's Law." *Journal of Fluid Mechanics* 602 (2008): 119-127.
- (7) Wu, X. L., R. Levine, M. Rutgers, H. Kellay, and W. I. Goldburg. "Infrared Technique for Measuring Thickness of a Flowing Soap Film." *Review of Scientific Instruments* 72, no. 5 (2001): 2467.
- (8) Schwartz, L.w, and R.v Roy. "Modeling Draining Flow in Mobile and Immobile Soap Films." *Journal of Colloid and Interface Science* 218, no. 1 (1999): 309-23.
- (9) Seiwert, Jacopo, Benjamin Dollet, and Isabelle Cantat. "Theoretical Study of the Generation of Soap Films: Role of Interfacial Visco-elasticity." *Journal of Fluid Mechanics* 739 (2013): 124-42.
- (10) Ropars, G., D. Chauvat, A. Le Floch, M. N. O'Sullivan-Hale, and R. W. Boyd. "Dynamics of Gravity-induced Gradients in Soap Film Thicknesses." *Physical Review Letters* 88, no. 23 (2006): 234104.
- (11) Gennes, P. G. De. "'Young' Soap Films." *Langmuir* 17, no. 8 (2001): 2416-419.
- (12) Sett, S., S. Sinha-Ray, and A. L. Yarin. "Gravitational Drainage of Foam Films." *Langmuir* 29, no. 16 (2013): 4934-947.

- (13) Prasad, V., and Eric R. Weeks. "Flow Fields in Soap Films: Relating Viscosity and Film Thickness." *Physical Review E* 80, no. 2 (2009): 026309.
- (14) Kellay, H., X-L. Wu, and W. I. Goldberg. "Experiments with Turbulent Soap Films." *Physical Review Letters* 74, no. 20 (1995): 3975-978.
- (15) Saulnier, Laurie, Frédéric Restagno, Jérôme Delacotte, Dominique Langevin, and Emmanuelle Rio. "What Is the Mechanism of Soap Film Entrainment?" *Langmuir* 27, no. 22 (2011): 13406-3409.
- (16) Adami, N., and H. Caps. "Surface Tension Profiles in Vertical Soap Films." *Physical Review E* 91, no. 1 (2015): 013007.
- (17) Sonin, A. A., A. Bonfillon, and D. Langevin. "Role of Surface Elasticity in the Drainage of Soap Films." *Physical Review Letters* 71, no. 14 (1993): 2342-345.
- (18) Casteletto, Valeria, Isabelle Cantat, Dipak Sarker, Richard Bausch, Daniel Bonn, and Jacques Meunier. "Stability of Soap Films: Hysteresis and Nucleation of Black Films." *Physical Review Letters* 90, no. 4 (2003): 048302.
- (19) Bonhomme, Oriane, Olivier Liot, Anne-Laure Biance, and Lydéric Bocquet. "Soft Nanofluidic Transport in a Soap Film." *Physical Review Letters* 110, no. 5 (2013): 054502.
- (20) Seiwert, Jacopo, Martin Monloubou, Benjamin Dollet, and Isabelle Cantat. "Extension of a Suspended Soap Film: A Homogeneous Dilatation Followed by New Film Extraction." *Physical Review Letters* 111, no. 9 (2013): 094501.
- (21) Sünderhauf, Gerhard, Hans Raszillier, and Franz Durst. "The Retraction of the Edge of a Planar Liquid Sheet." *Physics of Fluids* 14, no. 1 (2002): 198.
- (22) Berg, S., E. A. Adelizzi, and S. M. Troian. "Images of the Floating World: Drainage Patterns in Thinning Soap Films." *Physics of Fluids* 16, no. 9 (2004).
- (23) Berg, Steffen, Eric A. Adelizzi, and Sandra M. Troian. "Experimental Study of Entrainment and Drainage Flows in Microscale Soap Films." *Langmuir* 21, no. 9 (2005): 3867-876.
- (24) Adelizzi, Eric A., and Sandra M. Troian. "Interfacial Slip in Entrained Soap Films Containing Associating Hydrosoluble Polymer." *Langmuir* 20, no. 18 (2004): 7482-492.
- (25) Lioni-Addad, Sylvie, and Jean Marc Di Meglio. "Stabilization of Aqueous Foam by Hydrosoluble Polymers. 1. Sodium Dodecyl Sulfate-poly(ethylene Oxide) System." *Langmuir* 8, no. 1 (1992): 324-27.

- (26) Cohen-Addad, Sylvie, and Jean-Marc Di Meglio. "Stabilization of Aqueous Foam by Hydrosoluble Polymers. 2. Role of Polymer/surfactant Interactions." *Langmuir* 10, no. 3 (1994): 773-78.
- (27) Barnes, Howard A. *A Handbook of Elementary Rheology*. Aberystwyth: University of Wales, Institute of Non-Newtonian Fluid Mechanics, 2000.
- (28) Chen, Daniel T.n., Qi Wen, Paul A. Janmey, John C. Crocker, and Arjun G. Yodh. "Rheology of Soft Materials." *Annual Review of Condensed Matter Physics* 1, no. 1 (2010): 301-22.
- (29) Tabuteau, H., S. Mora, G. Porte, M. Abkarian, and C. Ligoure. "Microscopic Mechanisms of the Brittleness of Viscoelastic Fluids." *Physical Review Letters* 102, no. 15 (2009): 155501.
- (30) Nguyen, C. T., H. M. Gonnermann, Y. Chen, C. Huber, A. A. Maiorano, A. Gouldstone, and J. Dufek. "Film Drainage and the Lifetime of Bubbles." *Geochemistry, Geophysics, Geosystems* 14, no. 9 (2013): 3616-631.
- (31) Evers, L. J., S. Yu. Shulepov, and G. Frens. "Bursting Dynamics of Thin Free Liquid Films from Newtonian and Viscoelastic Solutions." *Physical Review Letters* 79, no. 24 (1997): 4850-853.
- (32) Prasad, V., and Eric R. Weeks. "Two-Dimensional to Three-Dimensional Transition in Soap Films Demonstrated by Microrheology." *Physical Review Letters* 102, no. 17 (2009): 178302.
- (33) Durian, D. J. "Foam Mechanics at the Bubble Scale." *Physical Review Letters* 75, no. 26 (1995): 4780-783.
- (34) Soller, Raenell, and Stephan A. Koehler. "Rheology of Steady-State Draining Foams." *Physical Review Letters* 100, no. 20 (2008): 208301.
- (35) Besson, Sébastien, Georges Debrégeas, Sylvie Cohen-Addad, and Reinhard Höhler. "Dissipation in a Sheared Foam: From Bubble Adhesion to Foam Rheology." *Physical Review Letters* 101, no. 21 (2008): 214504.
- (36) Janiaud, E., D. Weaire, and S. Hutzler. "Two-Dimensional Foam Rheology with Viscous Drag." *Physical Review Letters* 97, no. 3 (2006): 038302.
- (37) Kähärä, T., T. Tallinen, and J. Timonen. "Numerical Model for the Shear Rheology of Two-dimensional Wet Foams with Deformable Bubbles." *Physical Review E* 90, no. 3 (2014): 032307.
- (38) Segur, J. B., and Helen E. Oberstar. "Viscosity of Glycerol and Its Aqueous Solutions." *Industrial & Engineering Chemistry* 43, no. 9 (1951): 2117-120.

- (39) Anna, Shelley L., and Gareth H. Mckinley. "Elasto-capillary Thinning and Breakup of Model Elastic Liquids." *Journal of Rheology* 45, no. 1 (2001): 115.
- (40) Koplík, Joel, and Jayanth R. Banavar. "Extensional Rupture of Model Non-Newtonian Fluid Filaments." *Physical Review E* 67, no. 1 (2003): 011502.
- (41) Kivotides, Demosthenes, S. Louise Wilkin, and Theo G. Theofanous. "Entangled Chain Dynamics of Polymer Knots in Extensional Flow." *Physical Review E* 80, no. 4 (2009): 041808.
- (42) Fielding, Suzanne M. "Criterion for Extensional Necking Instability in Polymeric Fluids." *Physical Review Letters* 107, no. 25 (2011): 258301.
- (43) Gilet, T., T. Scheller, E. Reyssat, N. Vandewalle, and S. Dorbolo. "How Long Will a Bubble Be?" *ArXiv*, September 27, (2007): arXiv:0709.4412.
- (44) Petit, P., and AL Biance. "Bursting of Rigid Bubbles." *ArXiv*, October 11, (2013): arXiv:1310.3129.
- (45) Müller, Frank, Ulrike Kornek, and Ralf Stannarius. "Experimental Study of the Bursting of Inviscid Bubbles." *Physical Review E*, no. 6 (2007): 065302(R).
- (46) Tabuteau, H., S. Mora, G. Porte, M. Abkarian, and C. Ligoure. "Microscopic Mechanisms of the Brittleness of Viscoelastic Fluids." *Physical Review Letters* 102, no. 15 (2009): 155501.
- (47) Burton, J. C., F. M. Huisman, P. Alison, D. Rogerson, and P. Taborek. "Experimental and Numerical Investigation of the Equilibrium Geometry of Liquid Lenses." *Langmuir* 26, no. 19 (2010): 15316-5324.

## Non-printed sources

- (N1) "Largest Free Floating Soap Bubble (outdoors)." Guinness World Records. March 11, 2015. Accessed September 4, 2015.  
<http://www.guinnessworldrecords.com/world-records/largest-free-floating-soap-bubble>.
- (N2) "Welcome to Public Domain Pictures." Public Domain Pictures. Accessed March 10, 2016. <http://www.publicdomainpictures.net/>.
- (N3) "Water Treatment Systems & Process Technologies | GE Water." GE Water. Accessed March 14, 2016. <http://www.gewater.com/>.
- (N4) "Soap Bubble Wiki." Wikia. Accessed March 15, 2016.  
[http://soapbubble.wikia.com/wiki/Soap\\_Bubble\\_Wiki](http://soapbubble.wikia.com/wiki/Soap_Bubble_Wiki).